EFFECTS OF DIRECT-FED *BACILLUS PUMILUS* 8G-134 (NRRL B-50174) ON RUMINAL AND FECAL MICROBIAL POPULATIONS OF PRE- AND POSTPARTUM HOLSTEIN COWS

BY

SARA WESTERGAARD

THESIS

Submitted in partial fulfillment of the requirements
for the degree of Master of Science in Animal Sciences
in the Graduate College of the
University of Illinois at Urbana-Champaign, 2015

Urbana, Illinois

Master's Committee:

Professor Roderick I. Mackie, Chair, Director of Research
Professor Isaac K.O. Cann
Assistant Professor Felipe Cardoso

ABSTRACT

Direct-fed microbials (DFM) are used as feed supplements in agricultural industry to enhance animal health and performance. The effects of *Bacillus pumilus* 8G-134 (NRRL B-50174) as a feed supplement were investigated through 16S rRNA gene-based inferences about community structure changes, exploration of the intra-Genus taxonomic variance using oligotyping, as well as RNA-seq conducted on rumen and fecal microbial contents from lactating dairy cattle. These techniques aided in detecting changes in gastrointestinal tract microbial community populations. Phylogenetic 16S analysis identified the microbes present and bioinformatic techniques, i.e. Qiime and Oligotyping software, further elucidated the community structures. In order to further investigate the germination of *B. pumilus* spores in the rumen, a transcriptomic approach was employed. Oligotyping analysis revealed that certain *Bacillus* oligotypes were detected exclusively in DFM samples. These DFM oligotypes could be further differentiated between rumen fluid (RF) and fecal sample types. It remains unclear whether or not the spores germinated in the rumen, but the effects on the fecal microbiota are clear. The major finding in this work is a modulation of the Bacteroidetes in the fecal samples of the DFM fed cows. Previous reports have shown that an increased Firmicutes to Bacteroidetes ratio leads to increased energy harvest and an obese phenotype. In lactating dairy cows, the increased energy harvest from the colonic bacteria likely promotes enhanced milk production.

TABLE OF CONTENTS

CHAPTER 1: INTRODUCTION……1

CHAPTER 2: LITERATURE REVIEW…….2

CHAPTER 3: MATERIALS AND METHODS…….6

CHAPTER 4: RESULTS AND DISCUSSION…….10

CHAPTER 5: SUMMARY.....……..……..14

CHAPTER 6: FIGURES AND TABLES…...……...15

REFERENCES……..40

CHAPTER 1: INTRODUCTION

Bacillus pumilus is a gram positive, rod-shaped, aerobic, endospore-forming bacteria found prevalently in a variety of environments, plant, animal, and soil habitats. The system of germination regulation, the speed with which germination can occur, their role in health and disease, and their environmental niche have long been topics of research interest.

The ubiquity of this organism in their dormant state begs the question of whether the animal gut serves as a primary site for germination, outgrowth, and resporulation. There is mounting evidence confirming the ability of Bacillus endospores to do so, though the specific mechanisms remain unclear. As is such, several aspects of using Bacillus spores as direct-fed microbials (DFM) are also poorly understood: the benefits of using endospores rather than vegetative cells as a feed supplement, their effects on overall community structures in the gastrointestinal tract, and their effects on host health

The objectives of this experiment were to evaluate the effect of *Bacillus pumilus* 8G-134 (NRRL B-50174) as a feed supplement on rumen and fecal microbial communities. Molecular techniques were utilized to identify whole community changes in the gastrointestinal tract of the cow, including rumen and fecal communities. Phylogenetic 16S analysis identified the microbes present and bioinformatic techniques, i.e. Qiime and Oligotyping software, further elucidated the community structures. A transcriptomic approach was used to investigate the germination of *B. pumilus* spores in the rumen.

CHAPTER 2: LITERATURE REVIEW

DFM supplementation has been shown to improve growth performance, feed efficiency, milk production (34, 35). Spore probiotic supplementation may enhance host health by several mechanisms including, but not limited to: (i) decreasing the impacts of pathogenic or food-spoilage micro-organism overgrowth through competitive exclusion (ii) eliciting an immune response, and (iii) increasing nutrient availability (29) .

*Bacillu*s endospores can survive in a dormant state for extended periods in environments not conducive to cell growth. These spores exhibit minimal metabolic activity and resistance to environmental stresses, chemicals, and predation. Spores are composed of several layers not found in vegetative cells. The core of the spore contains all of the dipicolinic acid, spore enzymes, ribosomes, and DNA. Surrounding the core is an inner membrane. Many proteins involved in spore germination are found within or adjacent to this inner membrane. A germ cell wall and peptidoglycan (PG) structure coats the inner membrane. (25). These structures are similar in dormant spores and growing cell walls, but one major difference is the presence of muramic-acid- δ-lactam (MAL) in spore peptidoglycan structures. Vegetative cell wall PG consists of glycan strands of alternating N-acetylglucosamine (NAG) and N-acetylmuramic acid (NAM) residues. Each NAM residue has peptide side chains and 40% of them are cross-linked to parallel glycan strands. Half of the NAM residues lack side chains and are converted to MAL (26). Next, a permeable outer membrane lies under a spore coat, or exosporium. The spore coat provides significant resistance to environmental stressors such as UV radiation, exposure to high heat exposure, solvents, hydrogen peroxide, and lytic enzymes (22, 23, 24, 27).

These highly resistant spores may provide protection via competitive exclusion may contribute to host health. It was discovered in an experiment wherein fecal matter from adult

chickens was fed to newly hatched chicks and demonstrated their conferred resistance to *Salmonella infantitis* infections via large doses of salmonellae (31). Competitive exclusion occurs when two or more microorganisms in an ecological niche require the same limited resource for their survival. If a microorganism is introduced to a closed environment with a limited supply a particular resource, i.e. nutrient, receptor, location, etc., which another microorganism in that environment also requires, they cannot coexist and must compete for the resource. As is such, DFMs can benefit the host by outcompeting pathogens rendering them incapable of surviving in the gastrointestinal tract. Accordingly, DFM supplementation could benefit the host regardless of sporulation if, for instance, there were high enough quantities in the inoculum to prevent a pathogen from accessing gut mucosal receptors essential to their colonization.

Host-microbe interactions involved with DFM supplementation are poorly understood, but may involve mucosal interactions that limit pathogen attachment or reduce immune cell receptor availability. They could also be taken up by intestinal epithelial cells and elicit the release of pro-inflammatory compounds, promote the differentiation of regulatory immune cells, and/or stimulate the non-specific innate immune cell development. These immune responses are possible whether or not the DFM germinates in the gastrointestinal tract through interactions with spore coat structures (33). Research has shown the importance of *Bacillus subtilis* in the development of gut-associated lymphoid tissue (GALT) (4). Interestingly, these studies indicate that resporulation of Bacillus endospores, rather than vegetative cell growth, is the strongest contributing factor in GALT development (2, 6). GALT is a dense aggregation of isolated lymphoid follicles combined with a particular surrounding epithelium, follicle-associated epithelium (FAE), which together forms a Peyer's patch (PP). These PPs are complex

accumulations of pathogen recognizing, regulatory, and transporting immune cells that serve as a primary location for interactions between the gut microenvironment and lymphoid tissue. Collectively, GALT tissue is they are the largest collection of both aggregated and isolated lymphoid follicles and contains up to 70% of the host's immunocytes (33).

Nutrient substrate conversion does not occur in dormant spores, but there is mounting evidence of *Bacillus* spore germination in the gastrointestinal tract. There are numerous reports of spore counts exceeding the original inoculum excreted in feces of animals fed spore-supplemented diets. Mice inoculated orally with *Bacillus* spores excreted over three times the original inoculum. Spores were detectable for over a week following the treatment (4, 5). Research has shown that *Bacillus* spores are capable of germination, growth, and re-sporulation within the intestinal tract. *rrnO-tetC* mRNA, indicative of germination, and *cotB-tetC*, for germination were measured 18 hours following oral inoculation with 2×10^{10} spores. These mRNA signals from jejunum showed high levels of cell growth germination rates between 1% and 5% (2). A more sensitive assay was designed by fusing a genetically engineered chimeric *ftsH-lacZ* gene, which is only expressed in vegetative cells, in high levels to detect as few at 10^2 vegetative cells in the gut of orally inoculated mice. This confirmed significant levels of *Bacillus* spores germination in the jejunum and ileum. The evidence suggested that the spores may even briefly colonize the small intestine (5). Furthermore, though *Bacillus* spores preferentially germinate in aerobic environments, they have been shown to germinate and survive anaerobically via both fermentation and nitrate respiration (3,5,6,8).

Germination and outgrowth of Bacillus spores can directly alter nutrient availability via substrate conversion or by augmenting the overall rate or proportion of substrate utilization as they germinate and undergo cell growth relative to the environment prior to DFM

supplementation. Exposure to specific stimuli, or germinants, can lead to spore germination and outgrowth. As the spores convert into growing cells, they lose the dormancy and resistance properties that facilitate survival in hostile environments. There are several germinants including, but not limited to, high pressure, nutrients, pyridine-2,6-dicarboxylic acid (dipicolinic acid [DPA]) chelated 1:1 with calcium ion (CaDPA), dodecylamine, and peptidoglycan fragments (28).

They can also indirectly alter nutrient and substrate availability by altering the overall microbial community populations and, consequently, nutrient and substrate environment. A 16S rRNA gene sequence-based survey comparing the distal gut microbiota in adult mice with a homozygous mutation in their leptin gene (Lep^{ob}), which produces obesity, to the microbiota of lean littermates (*ob*/+ and +/+) showed that members of Bacteroidetes and Firmicutes contained over 90% of all phylogenetic variation in each group of mice. Relative abundances of Bacteroidetes in the obese phenotype (*ob/ob*) was 50% lower with corresponding increases in Firmicutes. The differences noted in *ob/ob* mice were unrelated to food consumption as even mice with reduced feed intake showed significantly higher body fat percentages. Increased relative abundances of body fat correlated to a higher ration of Firmicutes to Bacteroidetes. The same trend was observed in distal microbial populations of lean human participants. Furthermore, obese humans who lost weight by consuming fat- or carbohydrate- restricted low-calorie diets had increases in Bacteroidetes significantly correlated to the weight loss (21). Therefore, the overall proportions of these two phyla were associated with a significant difference in phenotypic traits.

CHAPTER 3: MATERIALS AND METHODS

Animal care and housing

All experimental procedures were conducted under protocol (No. 12231) approved by the University of Illinois (Urbana-Champaign) Institutional Animal Care and Use Committee. Forty-three (n=43) multiparous Holstein cows were assigned to two treatments in a completely randomized block design. Before calving, cows were housed in free stalls with individual Calan feed gates (American Calan Inc., Northwood, NH). Approximately 2 days before expected parturition, cows were moved to individual maternity pens until parturition. After parturition, cows were housed in tie stalls with mangers designed for measurement of feed intake. Cows were milked three times daily. During the experimental period, cows were fed at ad libitum intake. Diets (pre- and postpartum) were formulated to meet cows' requirements according to NRC (2001) and were delivered once daily as a total mixed ration (TMR).

Treatments and management

Cows in the DFM treatment (DFM, n=21) received 5.0 x 109 cfu of *Bacillus pumilus* 8G-134 (NRRL B-50174) DFM (Dupont Nutrition and Health, Waukesha, WI) in 28 g of medium, whereas cows in the control treatment (CON, n=22) received 28 g of medium as placebo. Treatments were mixed with 0.45 kg ground corn and top-dressed on the prepartum or lactation TMR once daily for each cow. Treatments were applied from 21 ± 1 days before expected calving date to 154 days after calving. Cows were randomly assigned to treatments and balanced for initial body weight (BW; 719 ± 9.59 kg vs 715 ± 9.78 kg for CON and DFM, respectively), parity (2.53 ± 0.42 vs 2.03 ± 0.36 for CON and DFM, respectively), and previous lactation (305 days) milk production (11,703 ± 543 kg vs 11,389 ± 473 kg for CON and DFM, respectively). In total, there were 4 cannulated cows (CONCAN, n=4) and 18 non-cannulated

(CONNON, n=18) cows in the control treatment and 5 cannulated cows (DFMCAN, n=5) and 16 non-cannulated cows in the (DFMNON, n=16) in the DFM treatment.

Sample collection

Fresh fecal (F) samples were obtained from the rectum of cannulated cows at four time points (28 and 7 days pre-parturition, 14 and 49 days post-parturition) and non-cannulated cows at two time points (14 and 49 days post-parturition). Each fecal sample was flash frozen in liquid nitrogen. Two fresh 50 ml rumen fluid (RF) samples were collected from cannulated cows at 2 hourly time points (0 and 4 hours post-feeding) at 4 time points (28 and 7 days pre-parturition, 14 and 49 days post-parturition). Of the samples collected, the first was flash frozen for subsequent DNA extraction and the second was stored immediately in ice and used to determine pH.

For the transcriptomic analysis, *Bacillus pumilus* 8G-134 spores and maltodextrin mix were placed in 5 capsules inside a nylon bag that was suspended in the rumen. The capsules were incubated in the rumen for 12 and 24 hours, bags were removed and capsules suspended in RNA protect. The samples were frozen in a dry ice ethanol bath and stored at -80°C until RNA extraction.

Bacterial DNA Extraction

To determine bacterial community composition of rumen fluid and/or fecal samples of cows fed the control or spore-supplemented diet, DNA was isolated from the rumen as previously described (7) and the feces using the MPBiomedicals FastDNA SPIN Kit for Soil (MP Biomedicals, CA) according to the manufacturer's instructions. DNA was eluted with 50 ul of water, quantified using the QUBIT dsDNA assay (Life Technologies, CA), and stored at -20°C for subsequent PCR reactions.

Barcoded PCR and 454 Pyrosequencing

Isolated bacterial DNA was barcoded and sequenced using 454 pyrosequencing technology. Primers targeting the V1 to V3 (1) hypervariable regions of the 16S rRNA gene were used for PCR amplification and barcoding as previously described (1). 454 pyrosequencing services were carried out at the Roy J Carver Biotechnology Center at the University of Urbana on a 454 FLX Titanium (454 Life Sciences—a Roche Company, Branford, CT, USA). The 16S pyrotags were sorted by their respective barcodes into libraries for analysis.

Sequence Analyses

Raw sequence data was analyzed using Qiime's software (10) package with the following exceptions to the default parameters: barcode correction was disabled, reverse primers were truncated, and sequences without reverse primers were excluded from downstream analyses. Quality filters were used to remove sequences exceeding 1000 base pairs or less than 200 base pairs in length, sequences with a quality score below 25, sequences with homopolymer runs exceeding 6 base pairs, and sequences with primer mismatches. OTU clustering was performed on reads passing quality filters and representative sequences were chosen using the Uclust method, based on sequence similarity with a threshold of 97%, and aligned with Greengenes core reference set (11, 14, 15, 16). Taxonomy was assigned using the RDP classifier with a confidence value threshold of 90% (17). OTU tables and phylogenetic trees were generated and used to perform alpha and beta diversity calculations (Figure 1) (18, 20).

Oligotyping

Sequences assigned to the *Bacillus* genus were identified and aligned to Greengene database with a sequence similarity threshold of 97% using PyNAST's (13) template-based aligner. Oligotyping software (9) was used to perform entropy analysis facilitating the

identification of nucleotide positions of interest. Nucleotide positions with the highest variation were decomposed using oligotyping pipeline into distinct groups converged oligotypes.

RNA sequencing

Purified RNA samples were sent to the W.M Keck Center for Comparative and Functional Genomics at the University of Illinois. The paired-end cDNA library was constructed and sequencing was performed using Illumina sequencing. The paired-end reads were trimmed for length and quality using CLC Genomics Workbench Version 5 (http://www.clcbio.com). Using the provided genome sequence as a template, RNA-Seq analysis was performed using the default settings in CLC Genomics Workbench.

CHAPTER 4: RESULTS AND DISCUSSION

Bacteria of the Firmicutes phylum dominated microbial communities in all fecal samples with abundances ranging from 52.6% to 66.0% of the total community (Figures 2A-2C). However, Firmicutes only constituted 14.1% to 15.8% of the total microbial community in RF samples, which contained high abundances of phylum Bacteroidetes (Fig. 2D). In fecal samples collected from DFM cattle, Actinobacteria counts ranged from 6.1% to 6.4% of the total community compared with of 18.1% to 20.7% in cattle fed diets without spore supplementation. Bacteroidetes were undetectable in the feces of DFM cattle, but constituted 14.1% to 19.1% of the total community in fecal samples obtained from cattle in the control group and 62.3% to 64.1% of rumen fluid samples. This taxonomic data suggests that *Bacillus* spore probiotic supplementation had a positive impact on Firmicutes and Actinobacteria communities while negatively influencing Bacteroidetes populations (Figures 2A-2H).

Abundances of bacteria from the *Bacillus* species ranged from 0.0 to 0.02% in all RF samples. *Bacillus* species represented 0.02% to 0.22% of the total in FDFMCAN compared to 0.1% to 0.11% in FCONCAN. FDFMNON collected 49 days after parturition contained the highest abundance of *Bacillus* at 0.99% of the total population (Figure 2I).

Measurements of ecological metrics revealed high levels of community richness, evenness, and diversity in all collected samples. The number of observations increased as the number of sequences per sample increased (Figure 3A). Similarly, the Shannon diversity index confirmed high diversity indices all sample types (Figure 3B). The evenness of the plots at higher species counts indicated that the sample distribution was an accurate representation of the population.

Unifrac distances were also used to assess the degree of dissimilarity between microbial communities via principal coordinate analysis (19). All CON samples were isolated and analyzed separately prior to analyzing the entire sample collection (Figure 4A). The RF and F samples clustered within their respective sample type regardless of dietary probiotic supplementation, as was evident by the distinct clustering along the first principal coordinate. There was no clear distinction between CON or DFM cattle (Figure 4B). This is not unexpected because probiotic supplementation was neither intended nor expected to affect the distance matrices or composition of gut population at levels significant enough to affect beta diversity measurements.

Oligotyping analysis was performed on *Bacillus* OTUs to further resolve any nucleotide variation. This technique allowed distinction of related sequence reads at a level that is not possible with Qiime software. 938 sequences from 65 samples containing 155 OTUs were extracted from the sequencing data for oligotyping analysis. An initial entropy analysis identified 5 oligotypes (Figures 5A-5B) with the highest peak occurring at the 74th nucleotide. Sequences containing a cytosine residue at this position were only detected in DFM samples. Sequences with gaps in the 74th nucleotide were more prevalent in CAN cows (Figure 5C). Entropy analysis of the 5 oligotypes revealed shared entropy peaks at the 56th and 82nd nucleotide positions (Figure 5C). Oligotyping was repeated with the 56th position, which had the highest mean entropy. This resulted in 14 different oligotypes. The T_{74} oligotype contained $T_{56}T_{74}$ and $A_{56}T_{74}$ (Figure 6A), the G oligotype contained $A_{56}G_{74}$, $G_{56}G_{74}$, and $T_{56}G_{74}$ (Figure 6B), the C oligotype contained $G_{56}C_{74}$ and $A_{56}C_{74}$ (Figure 6C), the gapped oligotype contained T_{56}-$_{74,}$ A_{56}-$_{74,}$ C_{56} -$_{74,}$ and G_{56}-$_{74}$ (Figure 6D), and the A oligotype contained $G_{56}A_{74}$, $A_{56}A_{74}$, and $T_{56}A_{74}$ (Figure 6E). The $T_{56}G_{74,}$ A_{56}-$_{74}$, $G_{56}C_{74}$, $A_{56}C_{74}$, C_{56} -$_{74}$, $T_{56}T_{74}$ T_{56}-$_{74}$, $G_{56}A_{74}$, and $A_{56}G_{74}$ were not detected in any RF samples. $T_{56}A_{74}$ was only detected in control rumen fluid samples while $T_{56}G_{74}$ and $G_{56}G_{74}$ were only in RFDFM samples. $T_{56}A_{74}$ and G_{56}

-$_{74}$ were seen more in FDFMNON samples compared to FDFMCAN (Figure 6F). This oligotyping step converged entropy values for all but the C_{74} oligotype (Figures 6C), which shared variation at the 56th position. The final oligotyping step returned 4 oligotypes that were only found in DFM cattle. $G_{56}C_{74}$ contained $T_{74}G_{56}C_{74}$ and $C_{74}G_{56}C_{74}$ and $A_{56}C_{74}$ contained $C_{74}A_{56}C_{74}$ and $T_{74}A_{56}C_{74}$. $T_{74}A_{56}C_{74}$ was only present in the RF and $T_{74}G_{56}C_{7}$ in the feces (Figures 7A-7B).

Oligotyping analysis revealed that oligotypes containing a cytosine residue at the 74th base position were detected exclusively in DFM samples. Sequences with guanidine at the same position accounted for significantly less of the rumen *Bacillus* sequences, occurring mainly in fecal samples. Further resolution of the sequences containing cytosine residues at position 74 showed guanine and adenine residues occurred equally at the 56th base pair, exclusively in DFMCAN samples. Those with adenine position 74 and cytosine at the 48th position were absent from FDFMCAN samples, while those with guanine at position 74 and cytosine at 48 were absent from RFDFM samples.

B. pumilus 8G-134 spores were incubated in the rumen for 12 and 24 hours and were rapidly frozen and stored for transcriptional analysis. Samples from cow 829, 8156, 8705, and 8718 were used for the analysis (n=4). RNA was extracted and the samples were submitted to the Keck center (University of Illinois at Urbana-Champaign) for sequencing. Paired end cDNA libraries were constructed and sequenced using Illumina HiSeq2500. The sequencing results were trimmed to remove primer sequences and poor quality reads resulting in approximately 31.2-33.1 million reads for each sample. *B. pumilus* reads were first mapped to the unannotated sequence in order to quantify reads that aligned to the genome. Approximately 9-12% of the reads mapped to the reference genome sequence. Reads were then mapped to the annotated genome sequence to detect matches to gene coding regions, excluding ribosomal and tRNA

sequences (Table 3). Analysis of the annotated mapping results showed that 99.98 to 99.99% of reads mapped to ribosomal RNA coding regions and 277 to 725 reads per sample mapped to non-ribosomal (NR) genes. BLAST analysis (12) of the prominent ribosomal peak (Fig. 8) determined that the region was not specific for *B. pumilus*. There were 242 genes which contained at least one read within the entire dataset. Only 11of these genes were detected in all samples (Table 2). Functional annotation of these genes revealed that they were related to translational control (translation elongation factors, chaperones), transcription (RNA polymerase), energy production (ATP Synthase), and sporulation, or displayed hypothetical-function genes. Spore protein coding genes were consistently detected.

The proportion of reads that aligned to non-ribosomal genes was low, despite the extensive amount of raw sequence data. Over 99.98% of the reads mapped to ribosomal genes even though ribosomal RNA subtraction was performed. The presence of reads aligning to genes involved in translation and transcription suggest that *B. pumilus* 8G-134 spores are capable of germination in the rumen; however, it is difficult to ascertain the mechanism of action with the results of this data analysis, owing to low non-ribosomal reads abundances and genome coverage for the dosed *B. pumilus* strain.

CHAPTER 5: SUMMARY

Summary

Though it is unclear whether or not the spores germinated in the rumen, the effects on the fecal microbiota are clear. Oligotyping analysis revealed that certain *Bacillus* oligotypes were detected exclusively in DFM samples. These DFM oligotypes could be further differentiated between RF and fecal sample types. The major finding in this work is a modulation of the Bacteroidetes in the fecal samples of the DFM fed cows. Previous reports have shown that an increased Firmicutes to Bacteroidetes ratio leads to increased energy harvest and an obese phenotype (21). In lactating dairy cows, the increased energy harvest from the colonic bacteria likely leads to enhanced milk production.

Limitations

Although the total number of samples collected and analyzed was large, the number of cannulated cows limited the analysis of rumen contents. Also, repeated exposure to oxic conditions during sample collection would inevitably alter the rumen environment in these animals, which is typically anaerobic.

The low proportion of reads and poor genome coverage of the RNA-seq analysis could be due to a number of different factors such as low inocula, lagged germination rates, the rapid submersion of capsular contents diluting the spores or vegetative cells, retention rates outside of the time range of sample collection, or repeated disruption of the anaerobic rumen environment during sample collection.

CHAPTER 6: FIGURES AND TABLES

Figure 1

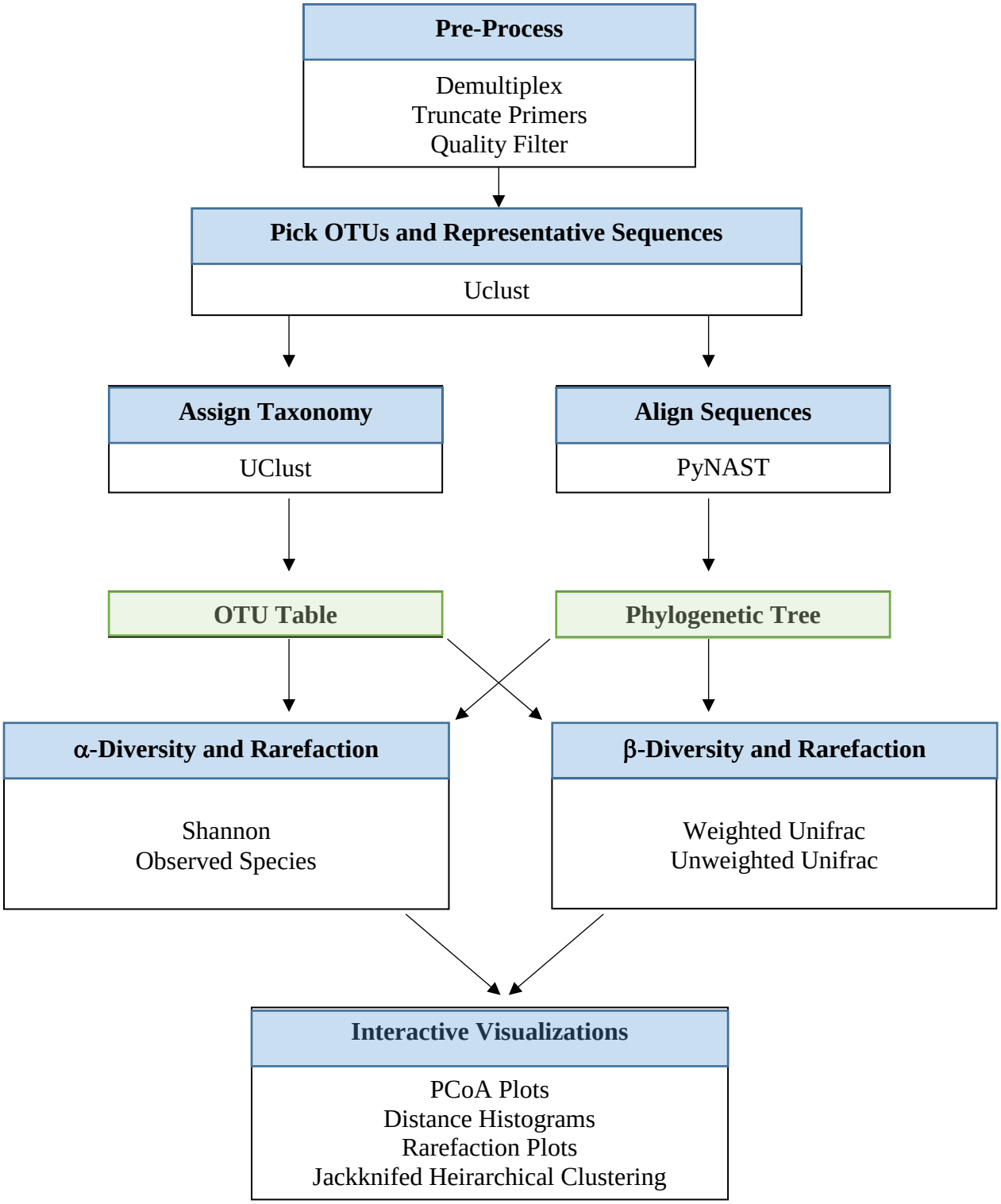

Figure 1. Qiime statistical analysis flowchart. A flowchart of the quality filtering and analysis pipeline of 16S rRNA genes.

Figure 2

A.

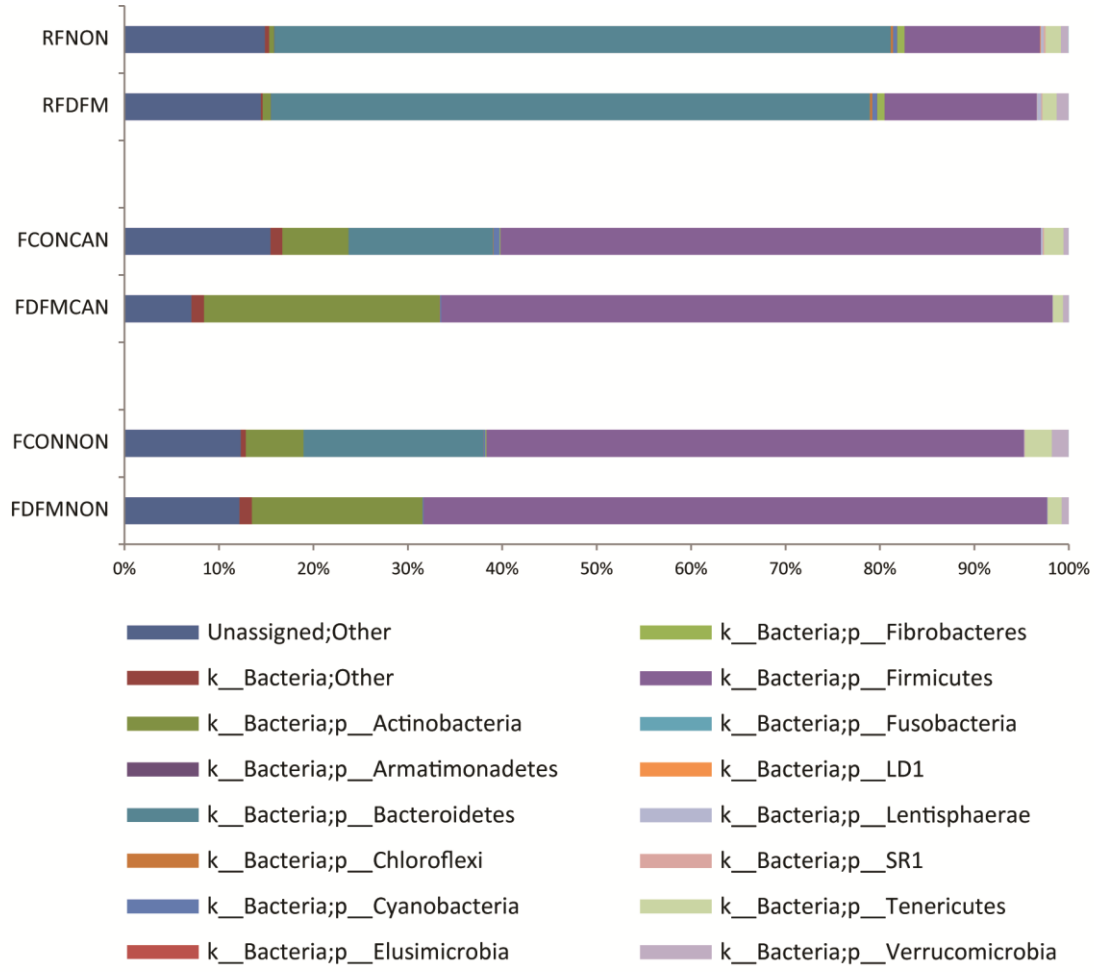

Taxon	FDFMNON	FCONNON	FDFMCAN	FCONCAN	RFDFM	RFNON
Unassigned;Other	12.2%	12.3%	5.9%	14.2%	14.2%	14.6%
k__Bacteria;Other	1.3%	0.5%	1.1%	1.2%	0.2%	0.5%
k__Bacteria;p__Actinobacteria	18.1%	6.1%	20.7%	6.4%	0.9%	0.5%
k__Bacteria;p__Armatimonadetes	0.0%	0.0%	0.0%	0.0%	0.0%	0.0%
k__Bacteria;p__Bacteroidetes	0.0%	19.1%	0.0%	14.1%	62.3%	64.1%
k__Bacteria;p__Chloroflexi	0.0%	0.0%	0.0%	0.0%	0.2%	0.2%
k__Bacteria;p__Cyanobacteria	0.1%	0.2%	0.1%	0.6%	0.5%	0.4%
k__Bacteria;p__Elusimicrobia	0.0%	0.0%	0.0%	0.0%	0.0%	0.0%
k__Bacteria;p__Fibrobacteres	0.0%	0.1%	0.0%	0.1%	0.8%	0.7%
k__Bacteria;p__Firmicutes	66.0%	56.9%	53.7%	52.6%	15.8%	14.1%
k__Bacteria;p__Fusobacteria	0.0%	0.0%	0.0%	0.0%	0.0%	0.0%
k__Bacteria;p__LD1	0.0%	0.0%	0.0%	0.0%	0.0%	0.1%
k__Bacteria;p__Lentisphaerae	0.0%	0.0%	0.0%	0.2%	0.4%	0.3%
k__Bacteria;p__SR1	0.0%	0.0%	0.0%	0.1%	0.1%	0.2%
k__Bacteria;p__Tenericutes	1.5%	2.9%	0.9%	1.9%	1.5%	1.6%
k__Bacteria;p__Verrucomicrobia	0.8%	1.8%	0.5%	0.5%	1.2%	0.8%
k__Bacteria;p__WPS-2	0.0%	0.0%	0.0%	0.0%	0.0%	0.1%

Figure 2 (cont.)

B.

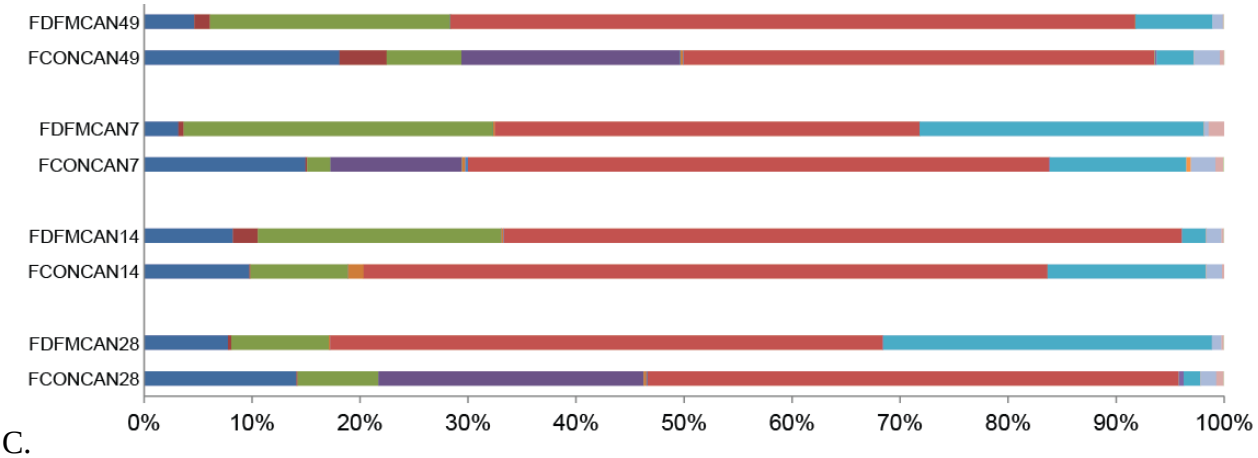

C.

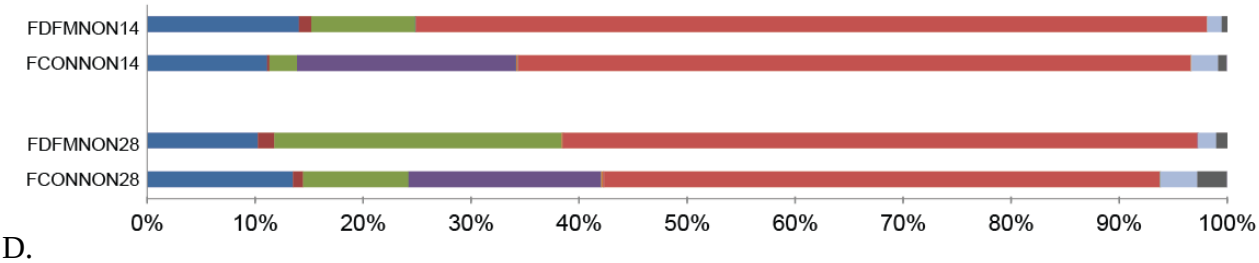

D.

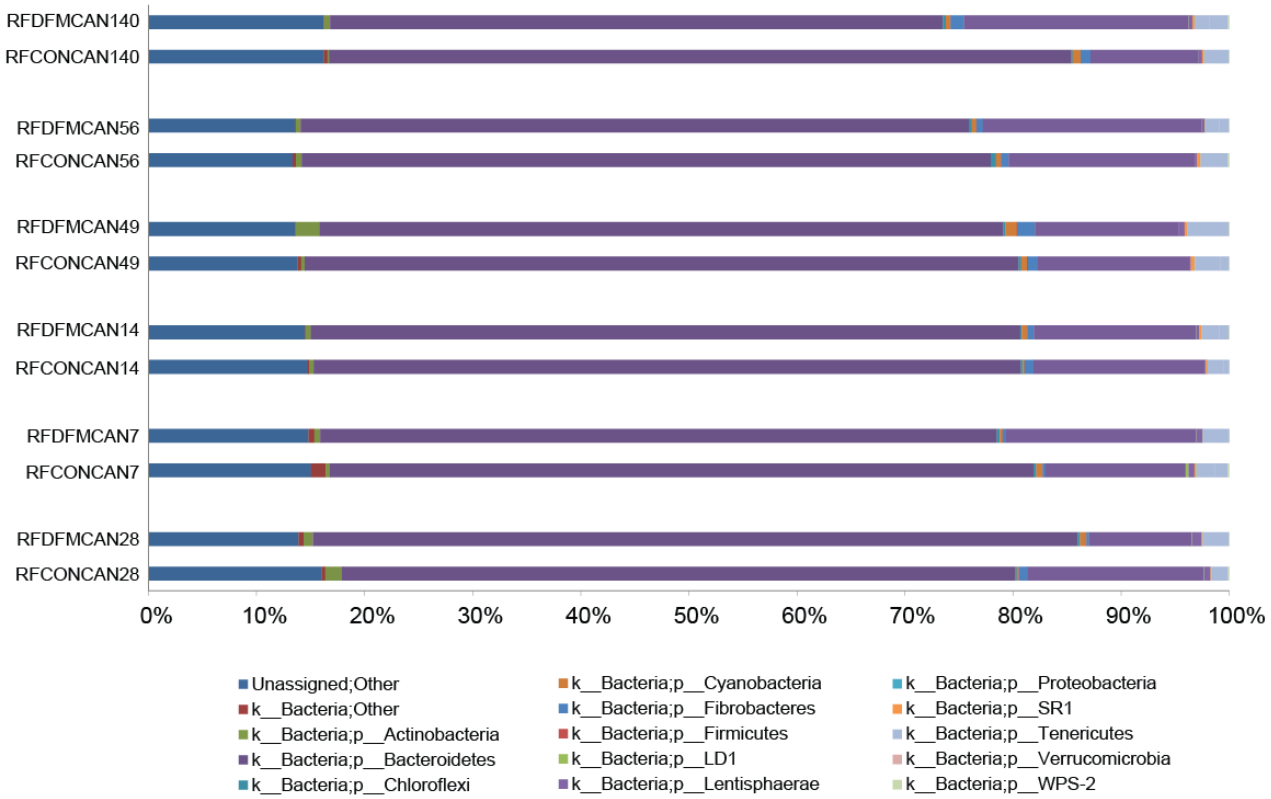

Figure 2 (cont.)

E.

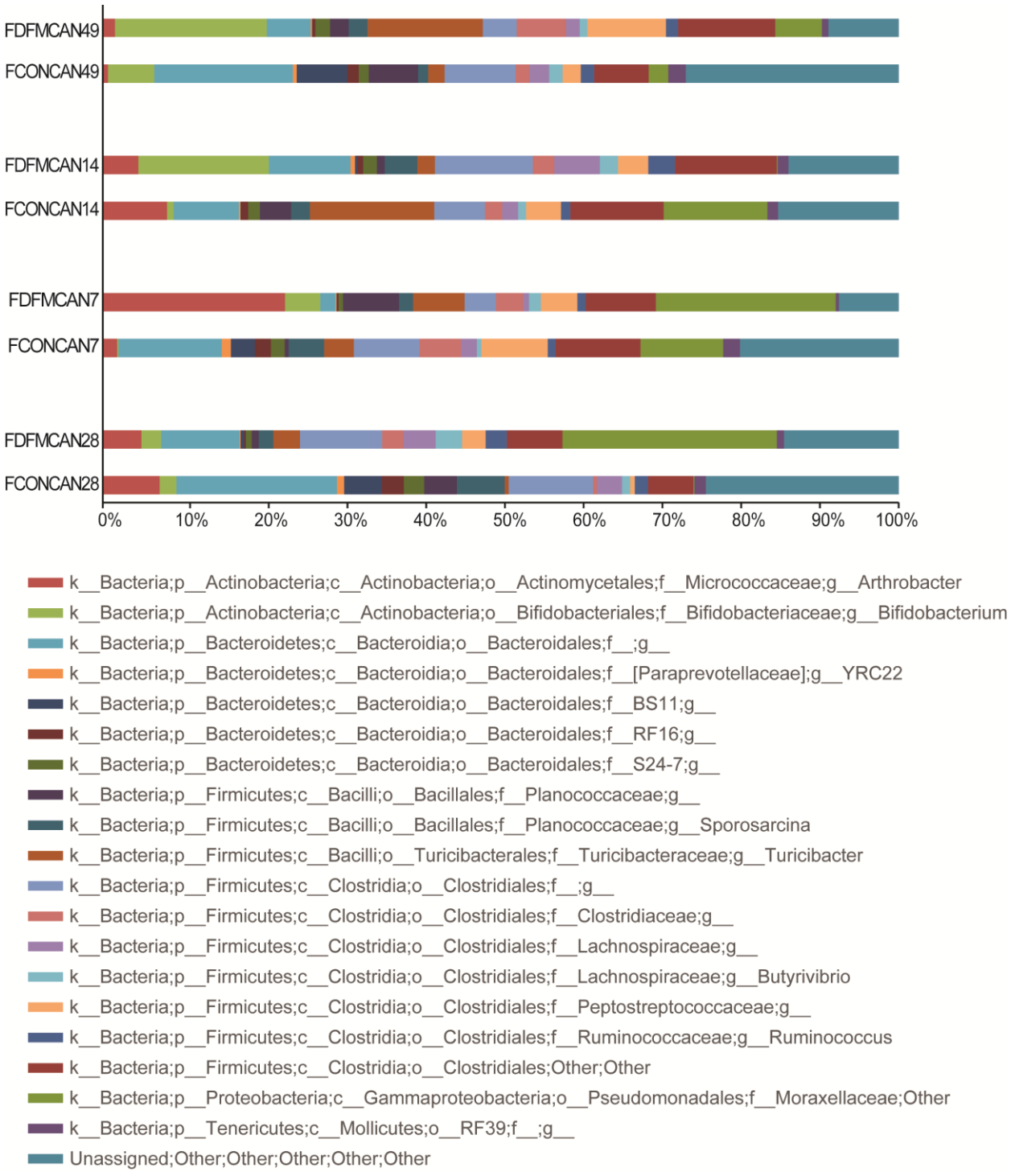

Figure 2 (cont.)
F.

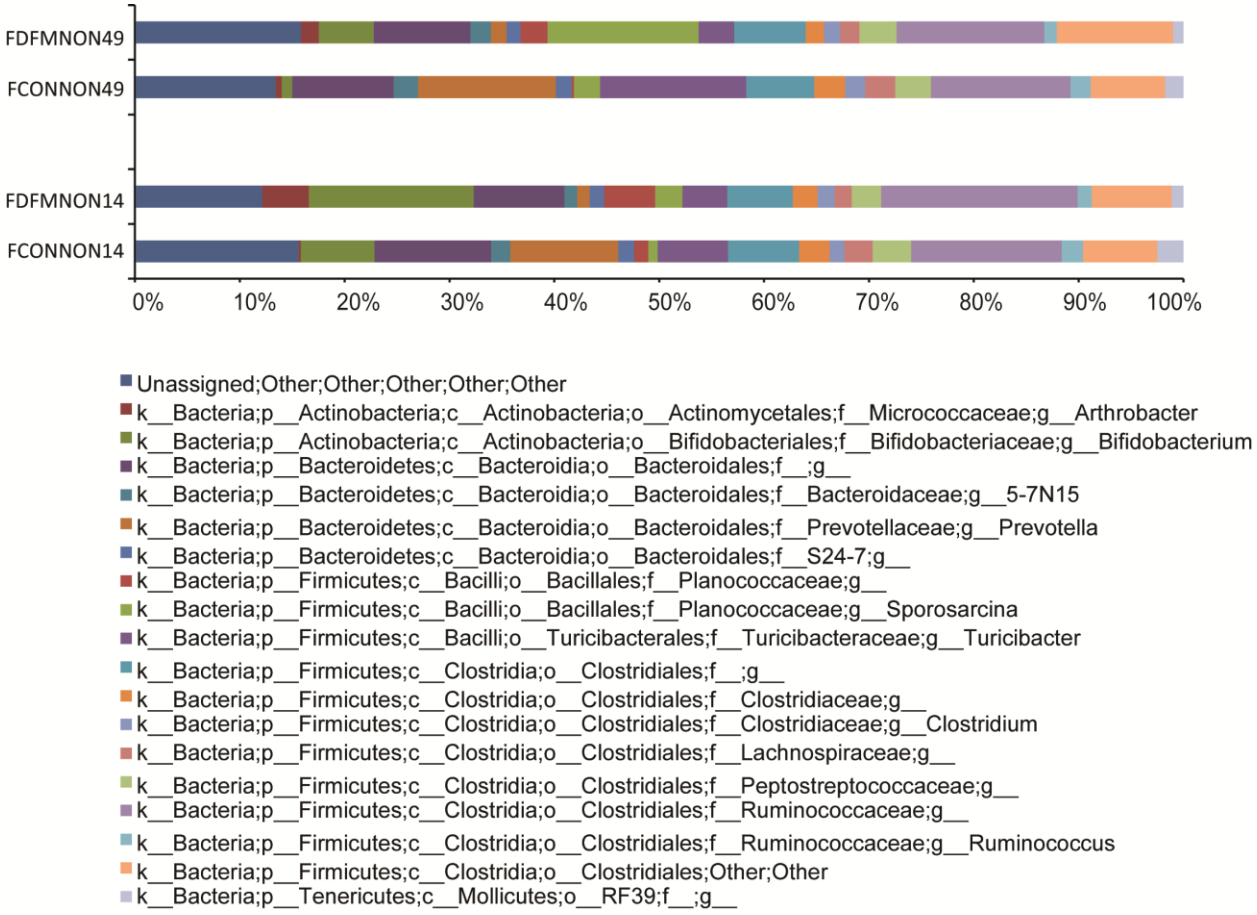

Figure 2 (cont.)
G.

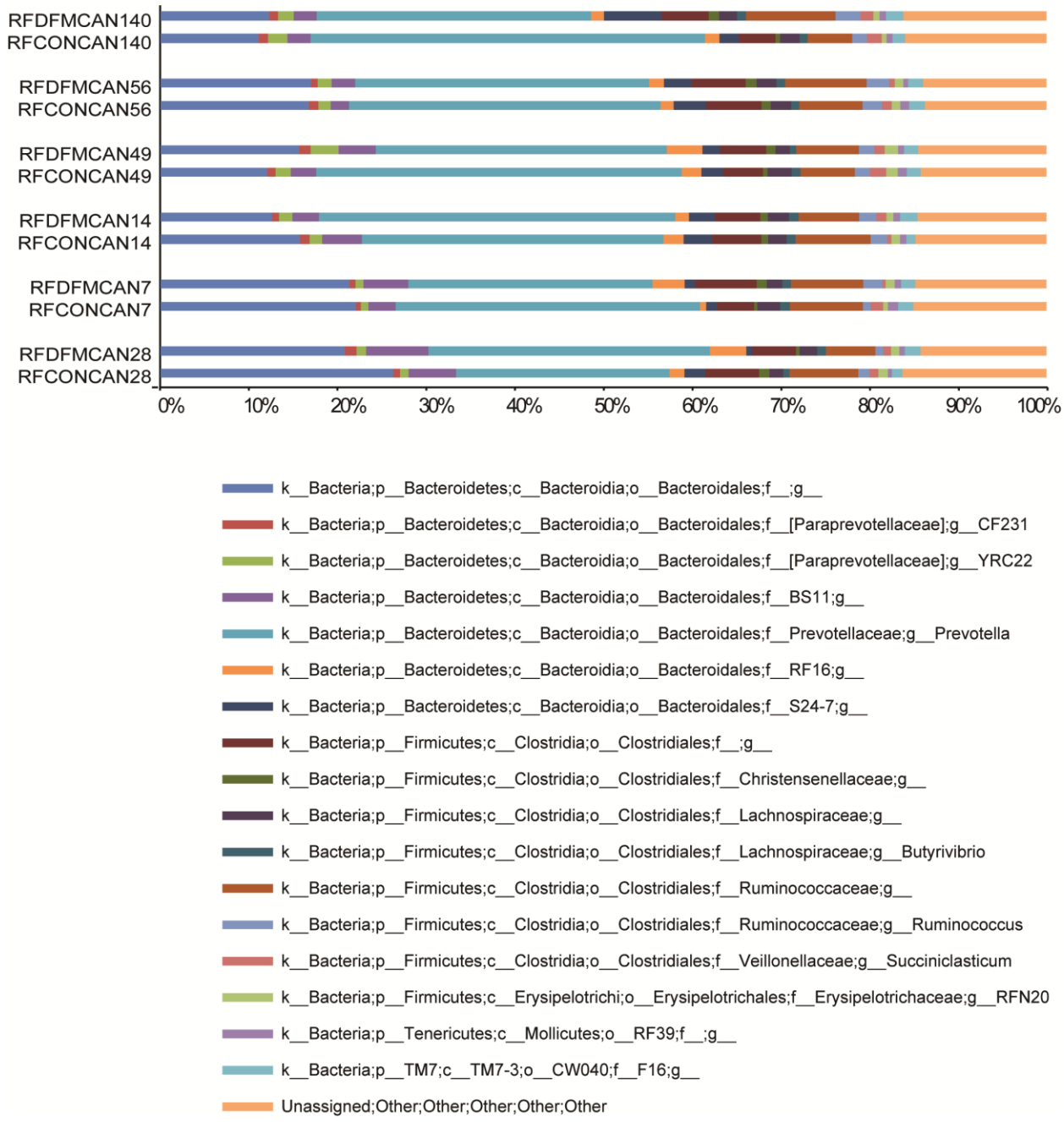

Figure 2 (cont.)

E

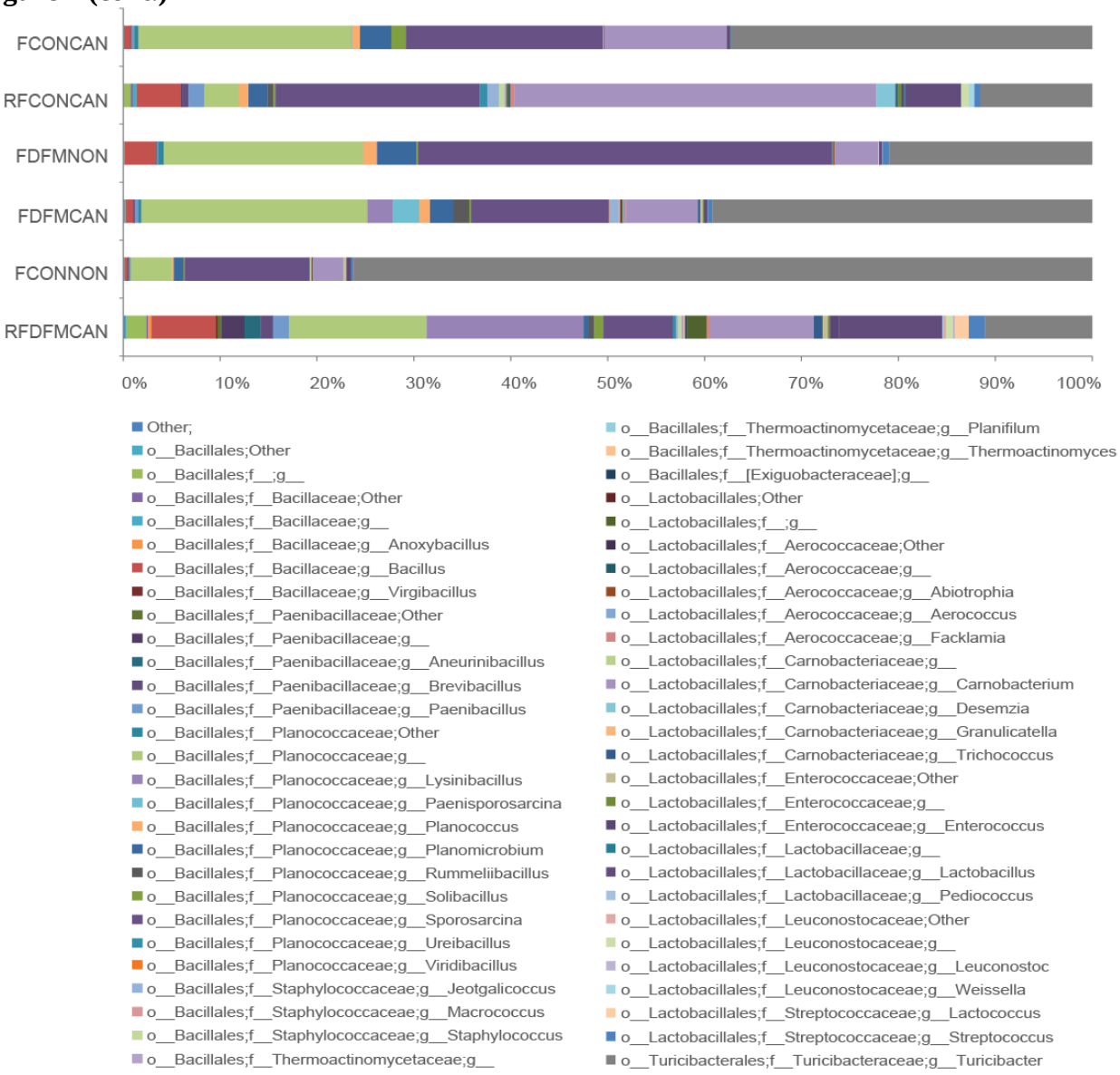

I.

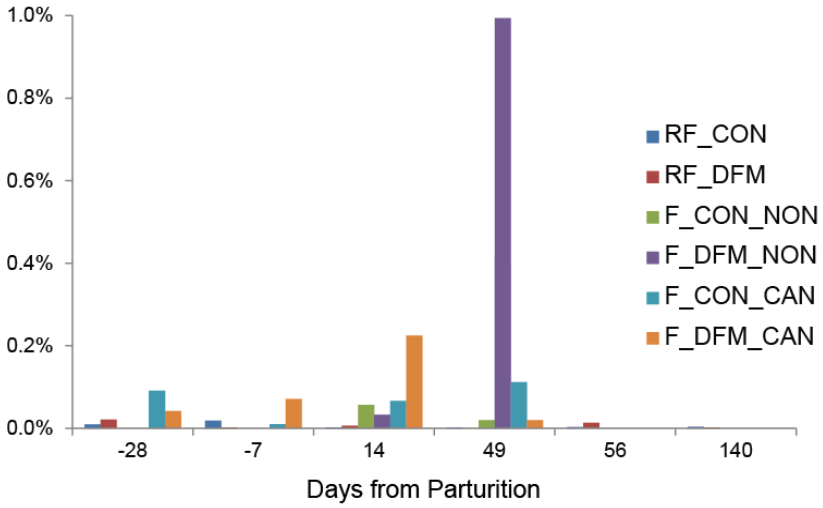

Figure 2 (cont.)

Figure 2. Taxonomic bacterial analyses. Phylum level taxonomic analysis of sample types in each treatment group at the phylum level (A). For all following bar graphs, detected taxa are listed in the y-axis and the x-axis shows relative abundances. Phylum-level taxonomic profiles in fecal samples (A), non-cannulated fecal samples (B), and rumen fluid samples (C), overall grouped according to time (D) Genus-level taxonomic analyses of cannulated fecal (E) non-cannulated fecal (F), rumen fluid (G), and samples at each sampling time and overall (H) are shown. Table showing the absolute abundance of *Bacillus* at the genus level (I). Abbreviations: RFDFM, rumen fluid from Direct Fed Microbial cattle; RFCON, rumen fluid from control cattle; FDFMCAN, feces from Direct Fed Microbial cannulated cattle; FCONCAN, feces from control cannulated cattle; FCONNON, feces from control non-cannulated cattle; FDFMNON, feces from Direct Fed Microbial non-cannulated cattle. The numbers following abbreviations the number of days from parturition: 28, twenty-eight days pre-parturition; 7, seven days pre-parturition; 14, fourteen days post-parturition; 49, forty-nine days post-parturition; 56, fifty-six days post-parturition; and 140, one hundred and forty days post-parturition.

Figure 3

A.

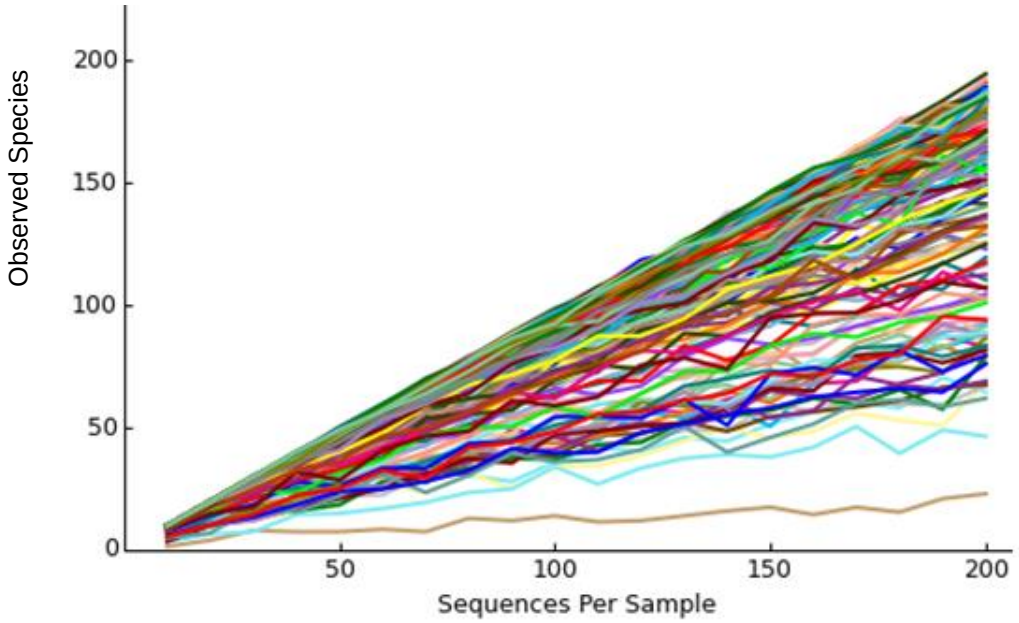

B.

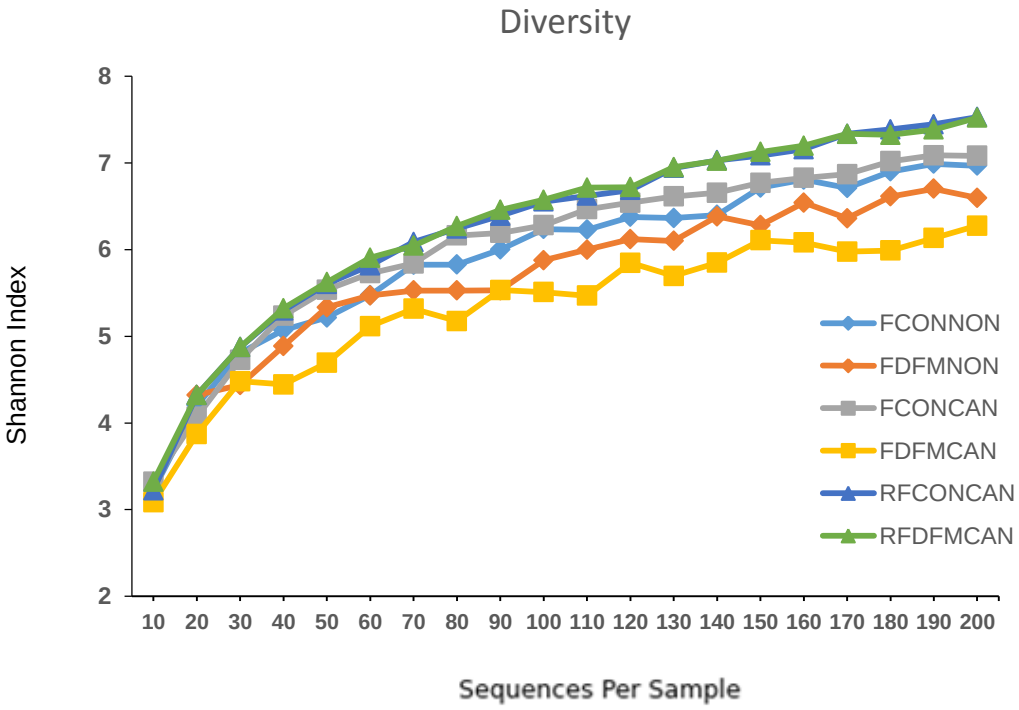

Figure 3. Alpha diversity metrics. Total observed species (A) and Shannon diversity indices (B), evened out as the number of sequences per sample increased. Abbreviations: RFDFM, rumen fluid from Direct Fed Microbial cattle; RFCON, rumen fluid from control cattle; FDFMCAN, feces from Direct Fed Microbial cannulated cattle; FCONCAN, feces from control cannulated cattle; FCONNON, feces from control non-cannulated cattle; FDFMNON, feces from Direct Fed Microbial non-cannulated cattle.

Figure 4

A.

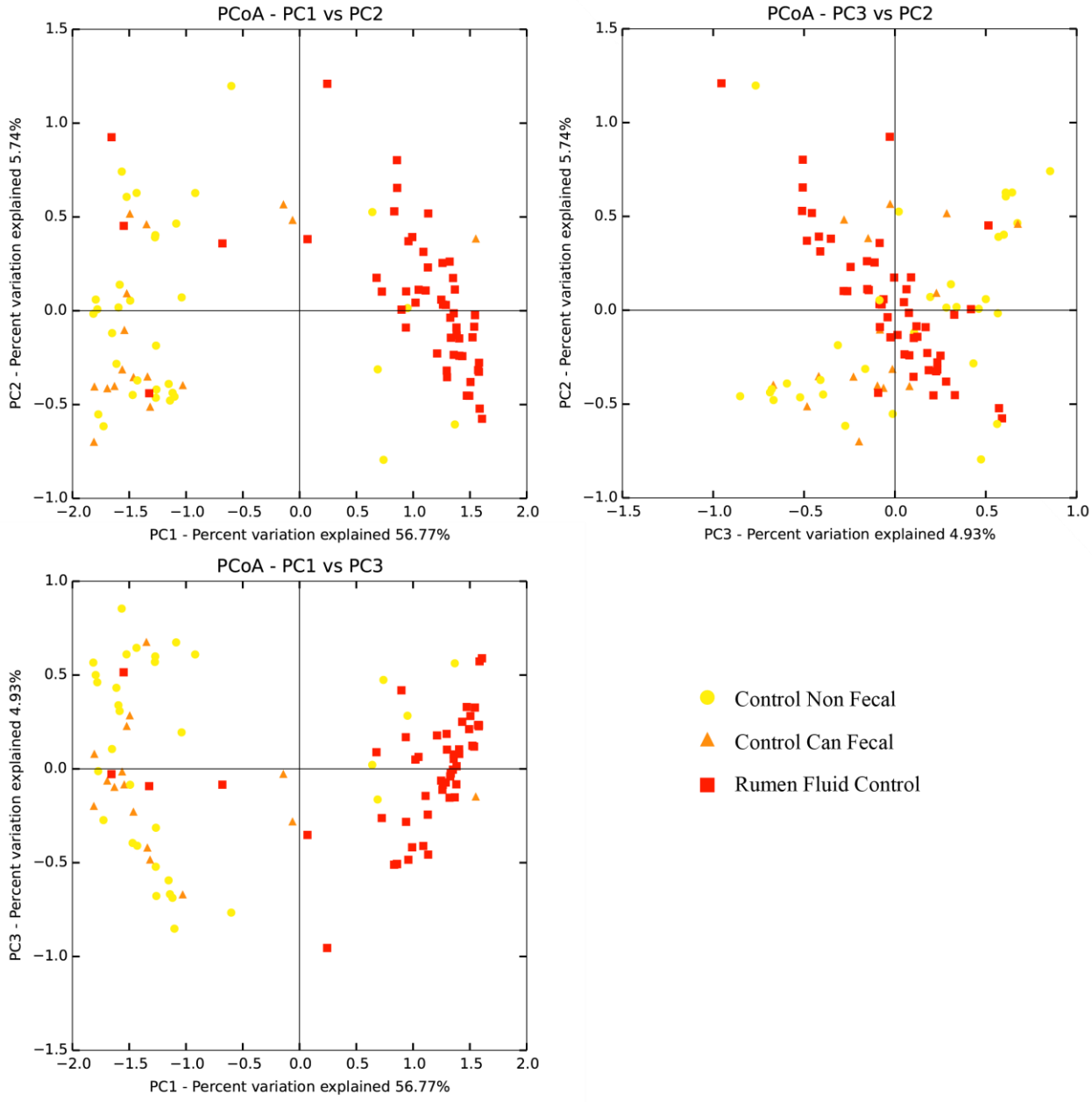
PCoA - PC1 vs PC2
PC2 - Percent variation explained 5.74%
PC1 - Percent variation explained 56.77%
PCoA - PC3 vs PC2
PC2 - Percent variation explained 5.74%
PC3 - Percent variation explained 4.93%
PCoA - PC1 vs PC3
PC3 - Percent variation explained 4.93%
PC1 - Percent variation explained 56.77%
Control Non Fecal
Control Can Fecal
Rumen Fluid Control

Figure 4 (cont.)
B.

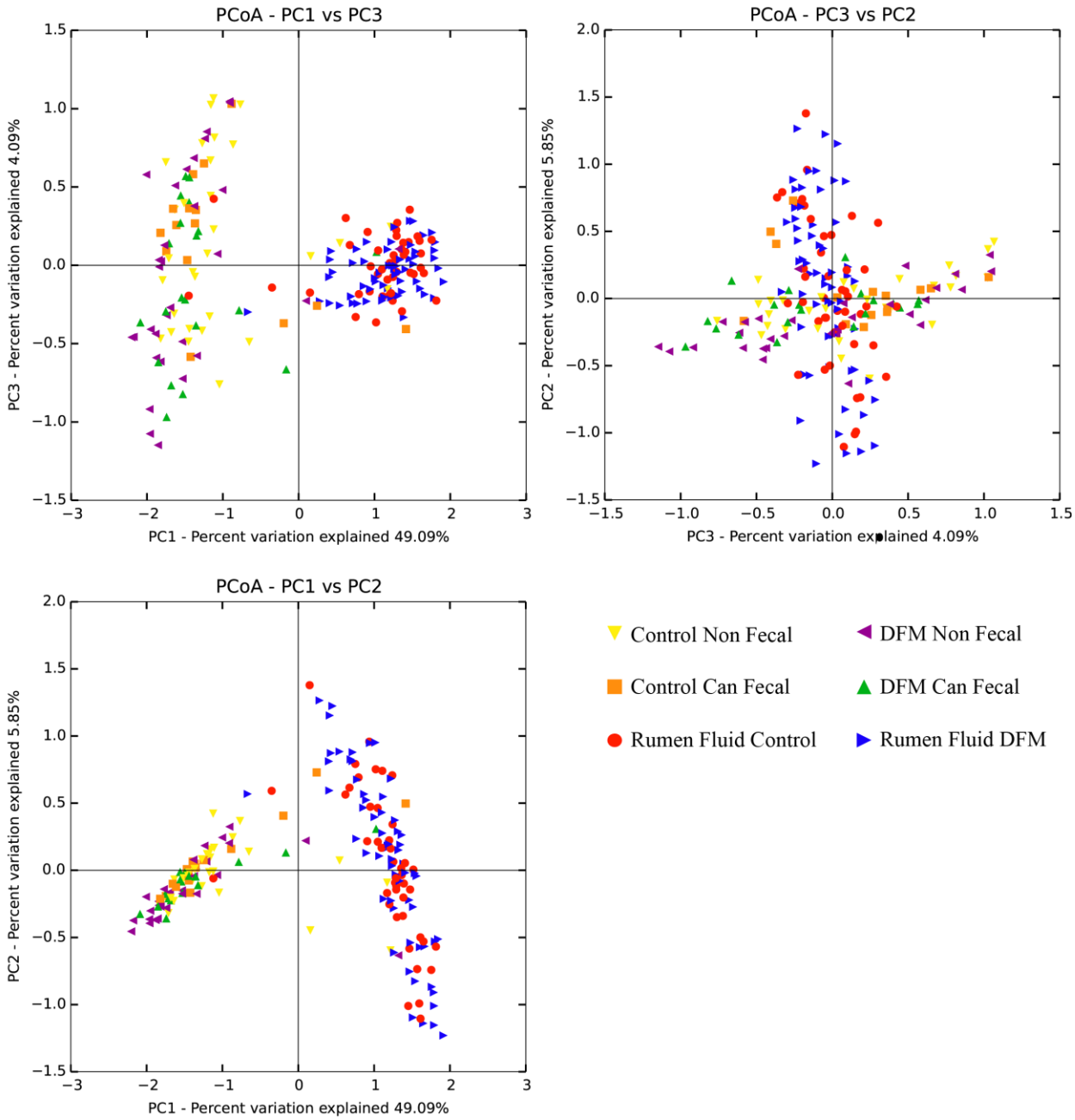

Figure 4. Beta diversity metrics. Sample type- and treatment-specific differences in bacterial ecology were analyzed. Multidimensional scaling (MDS) was used to generate a principal coordinate analysis (PCoA) matrix representing dissimilarities between bacterial lineages. Samples from the control treatment group (A) and collective samples (B) are shown. Clustering was observed relative to fecal or RF sample types regardless of treatment group. Abbreviations: NON, non-cannulated; CAN, cannulated.

Figure 5

A.

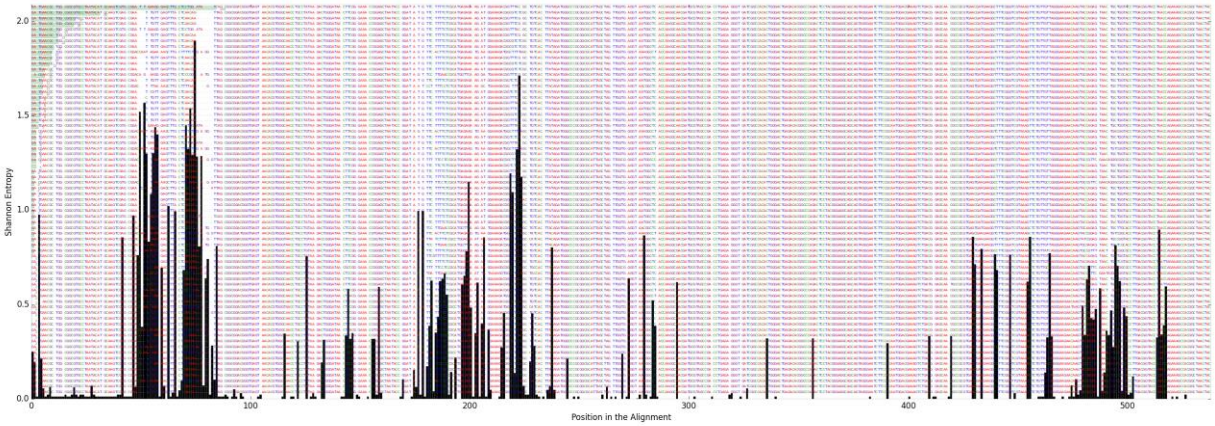

B.

Base Position	Entropy
49	1.5208
51	1.5681
72	1.5380
74	1.8982
222	1.7107

Figure 5 (cont.)
C.

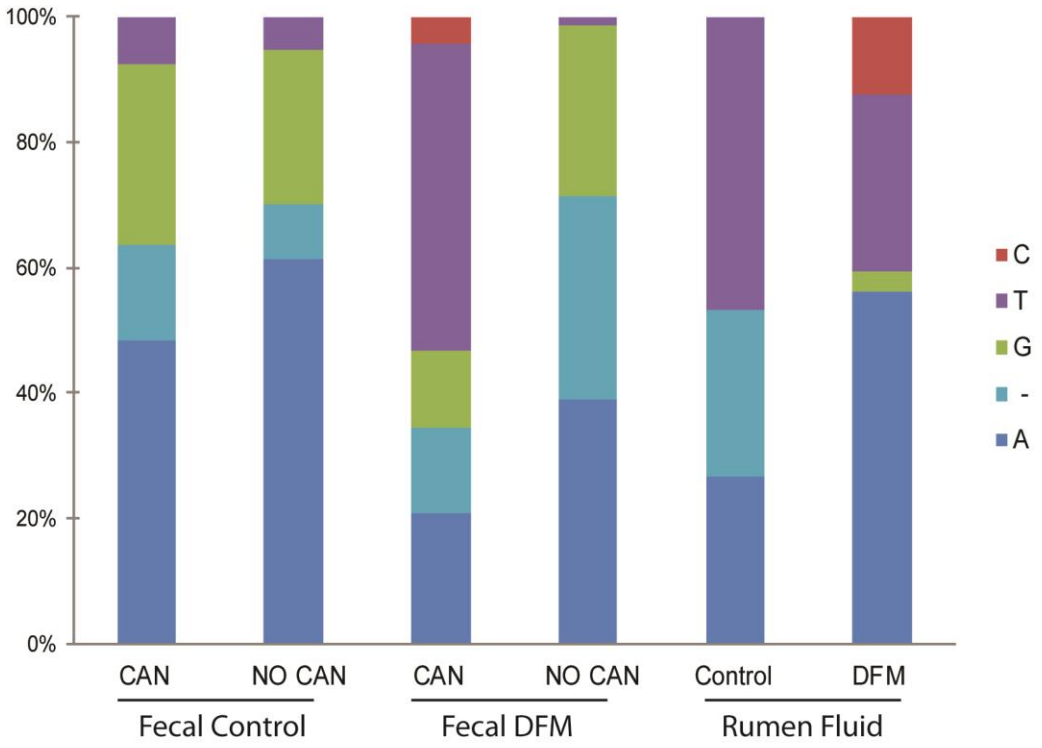

Group	Sample Type	A	-	G	T	C
Control	Rumen Fluid	26.7%	26.7%	0.0%	46.7%	0.0%
	Fecal Cannulated	48.5%	15.2%	28.8%	7.6%	0.0%
	Fecal Non-Cannulated	61.4%	8.8%	24.6%	5.3%	0.0%
DFM	Rumen Fluid	56.3%	0.0%	3.1%	28.1%	12.5%
	Fecal Cannulated	20.8%	13.5%	12.5%	49.0%	4.2%
	Fecal Non-Cannulated	38.8%	32.4%	27.2%	1.5%	0.0%

Figure 5 (cont.)
D.

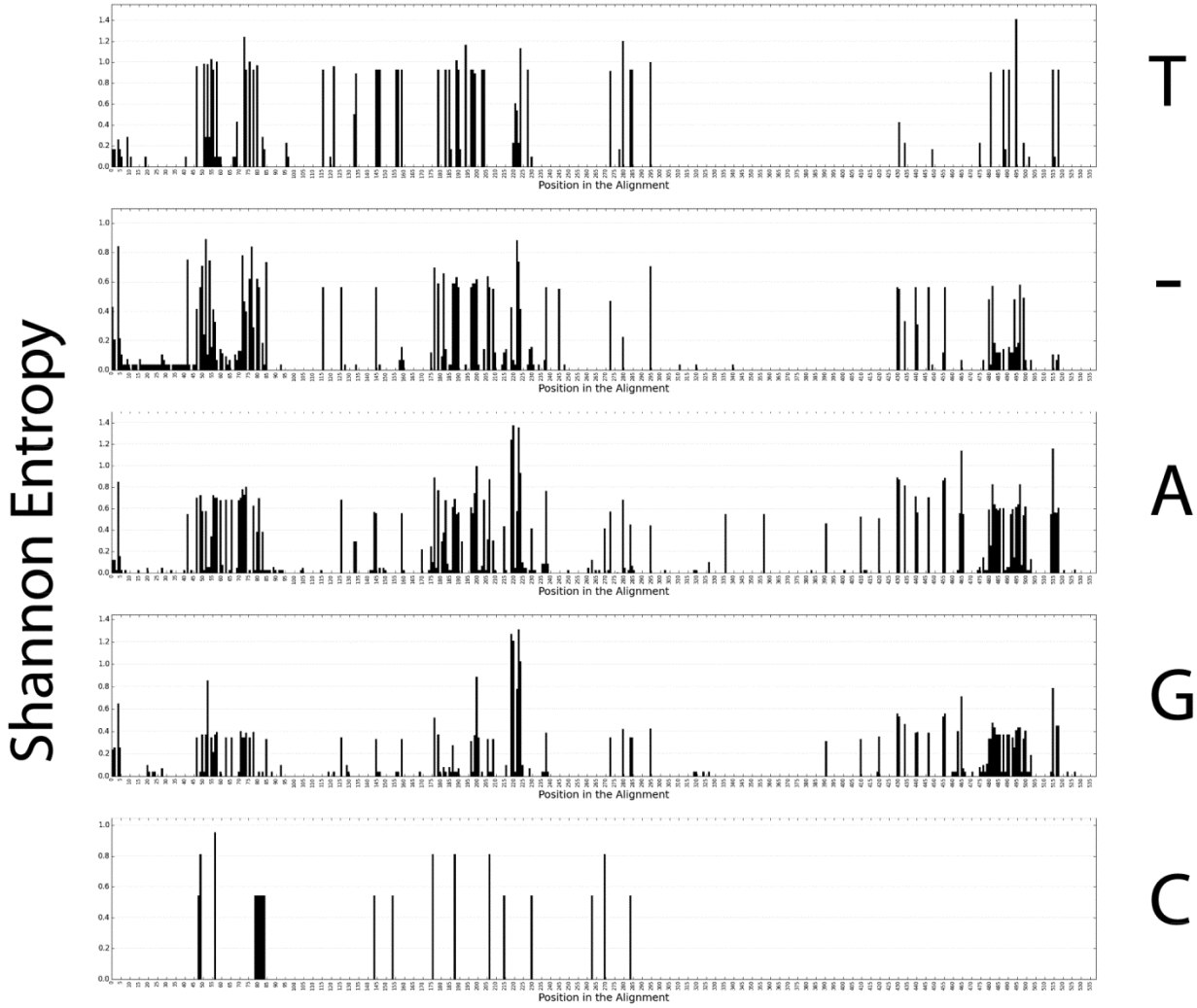

Figure 5. Initial Shannon entropy profiles and oligotyping analysis of *Bacillus* reads at base position 74. Shannon entropy analysis results on 938 *Bacillus* reads aligned, padded with gaps, and trimmed to a uniform length of 538 nucleotides. The entropy values for each position are represented by bars (A) and a table with showing the 5 base positions with the highest entropy values (B). The distribution of oligotypes at position 74 among samples is shown (C), with the corresponding Shannon entropy values represented by bars (D).

Figure 6

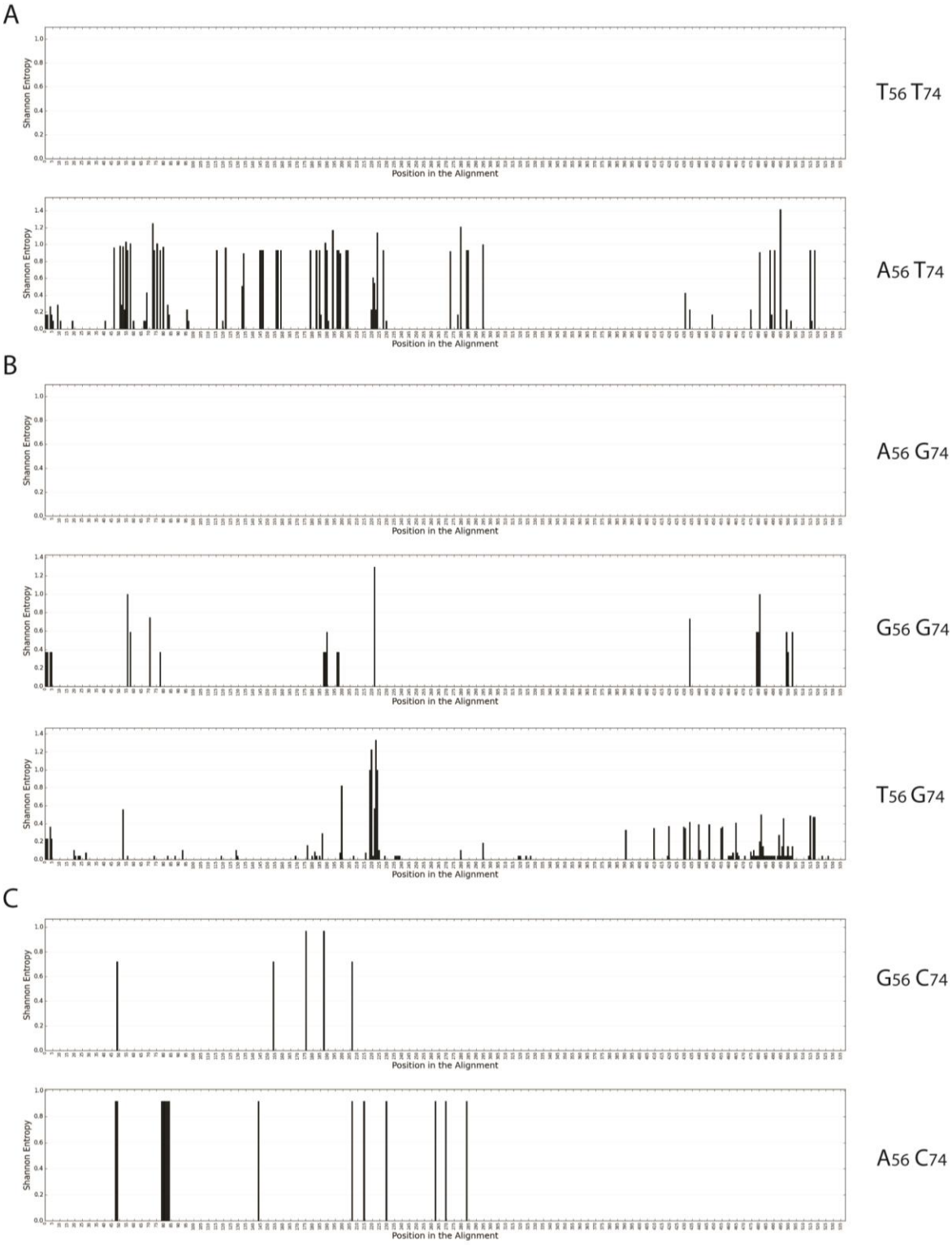
A
Shannon Entropy
Position in the Alignment
T56 T74
A56 T74
B
A56 G74
G56 G74
T56 G74
C
G56 C74
A56 C74

Figure 6 (cont.)

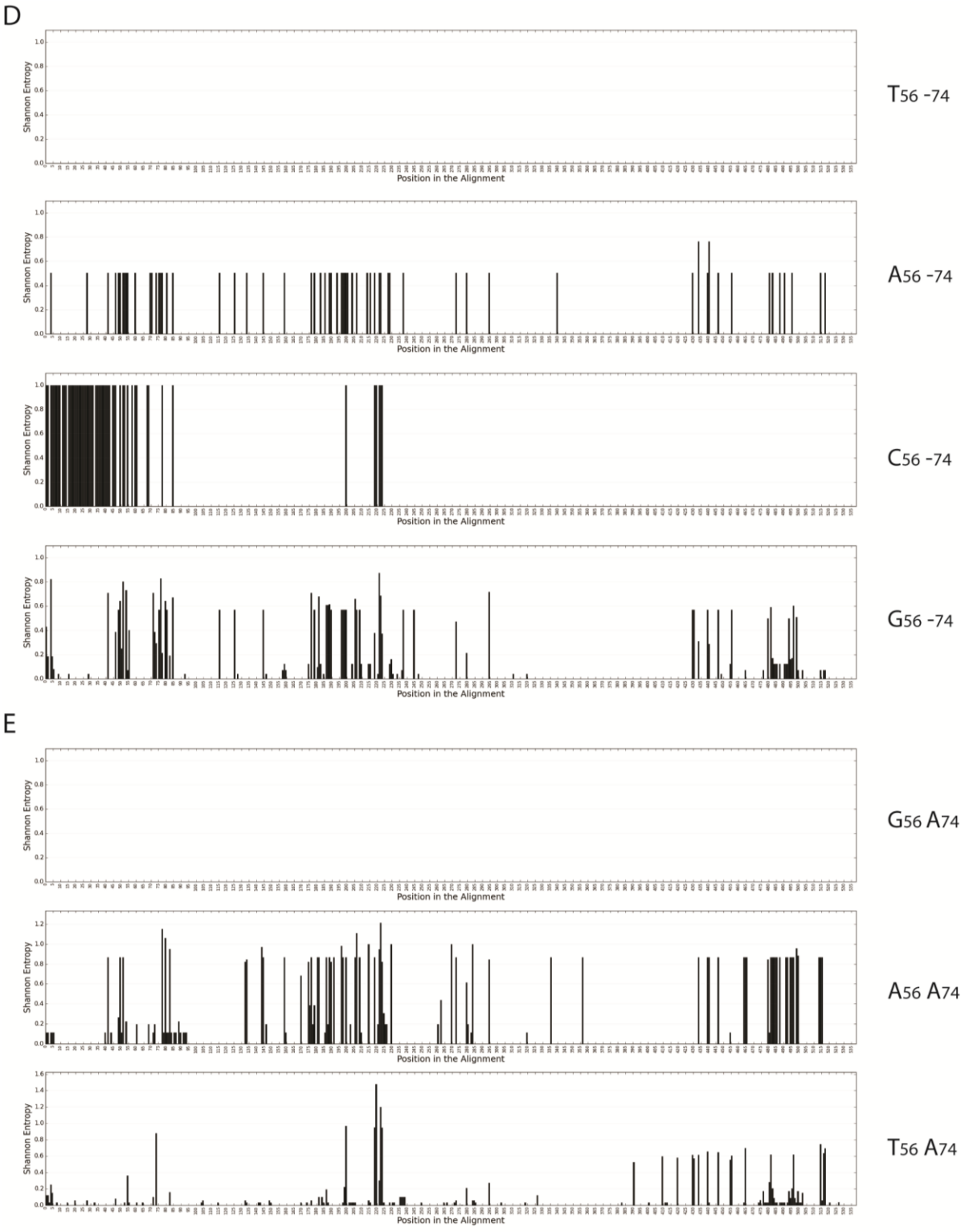

Figure 6 (cont.)

F.

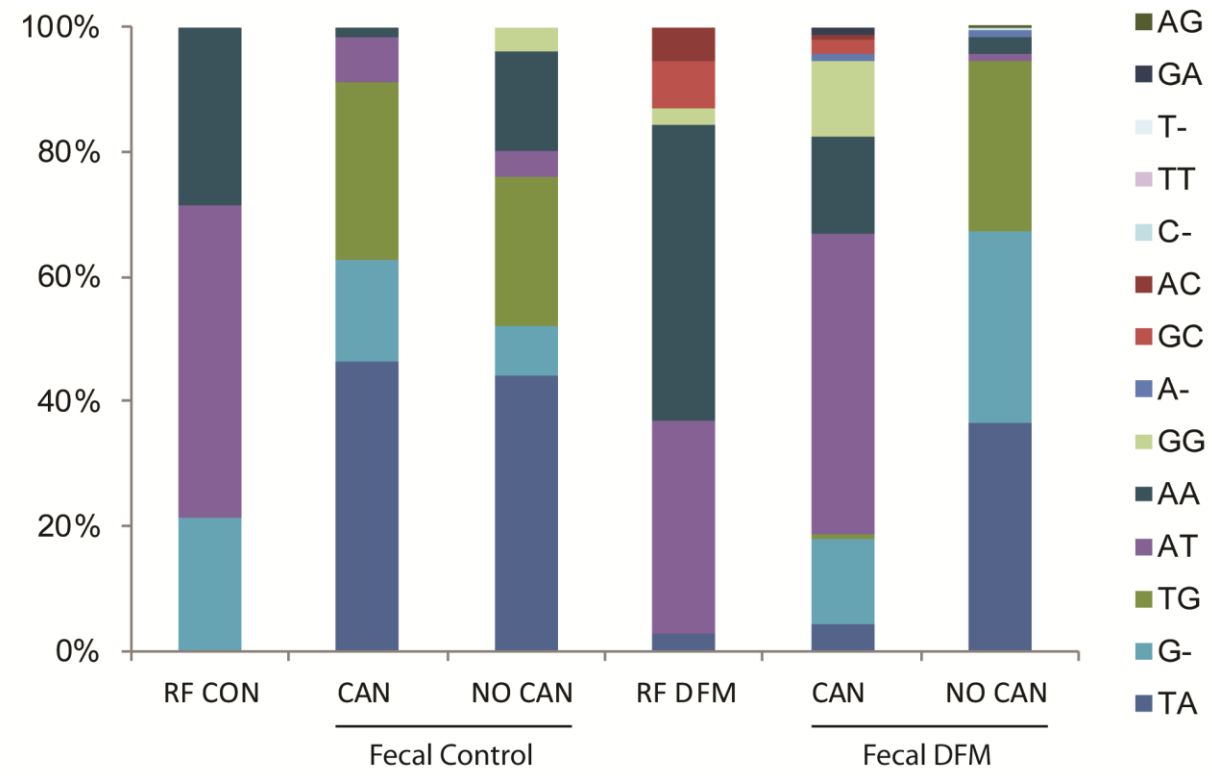

Group	Sample Type	TA	G-	TG	AT	AA	GG	A-	GC	AC	C-	TT	T-	GA	AG
Control	RFCON	0.0%	21.4%	0.0%	50.0%	28.6%	0.0%	0.0%	0.0%	0.0%	0.0%	0.0%	0.0%	0.0%	0.0%
	FCONCAN	46.3%	16.4%	28.4%	7.5%	1.5%	0.0%	0.0%	0.0%	0.0%	0.0%	0.0%	0.0%	0.0%	0.0%
	FCONNON	44.0%	8.0%	24.0%	4.0%	16.0%	4.0%	0.0%	0.0%	0.0%	0.0%	0.0%	0.0%	0.0%	0.0%
DFM	RFDFM	2.6%	0.0%	0.0%	34.2%	47.4%	2.6%	0.0%	7.9%	5.3%	0.0%	0.0%	0.0%	0.0%	0.0%
	FDFMCAN	4.4%	13.3%	1.1%	47.8%	15.6%	12.2%	1.1%	2.2%	1.1%	0.0%	0.0%	0.0%	1.1%	0.0%
	FDFMNON	36.5%	30.8%	27.1%	1.3%	2.4%	0.0%	1.2%	0.0%	0.0%	0.3%	0.1%	0.1%	0.0%	0.1%

Figure 6. Shannon entropy profiles and iterative oligotyping analysis of *Bacillus* reads at base positions 56 and 74. The Shannon entropy values for the T (A), G (B), C (C), gapped (D), and A (E) oligotypes are represented by bars. The distribution of oligotypes among samples is shown (F). Abbreviations: RFDFM, rumen fluid from Direct Fed Microbial cattle; RFCON, rumen fluid from control cattle; FDFMCAN, feces from Direct Fed Microbial cannulated cattle; FCONCAN, feces from control cannulated cattle; FCONNON, feces from control non-cannulated cattle; FDFMNON, feces from Direct Fed Microbial non-cannulated cattle.

Figure 7

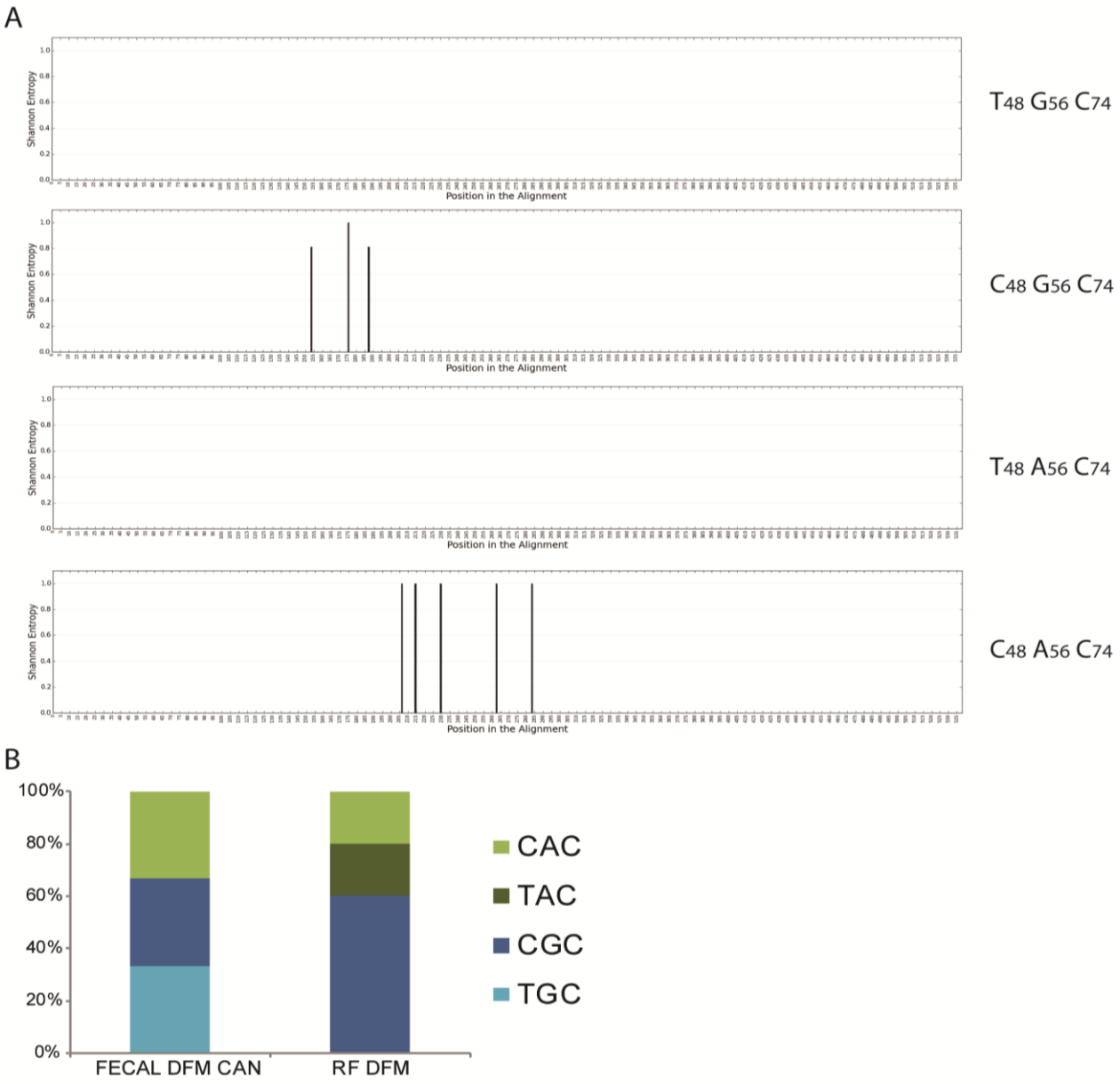

Group	Sample Type	TGC	CGC	TAC	CAC
DFM	Fecal Cannulated	33.3%	33.3%	0.0%	33.3%
	Rumen Fluid	0.0%	60.0%	20.0%	20.0%

Figure 7. Shannon entropy profiles and oligotyping analysis of Bacillus reads at base positions 48, 56, and 74. Shannon entropy values (A) and oligotype distribution among samples (B) of converged oligotypes at three variable positions. Abbreviations: RFDFM, rumen fluid from Direct Fed Microbial cattle; RFCON, rumen fluid from control cattle; FDFMCAN, feces from Direct Fed Microbial cannulated cattle; FCONCAN, feces from control cannulated cattle; FCONNON, feces from control non-cannulated cattle; FDFMNON, feces from Direct Fed Microbial non-cannulated cattle.

Figure 8

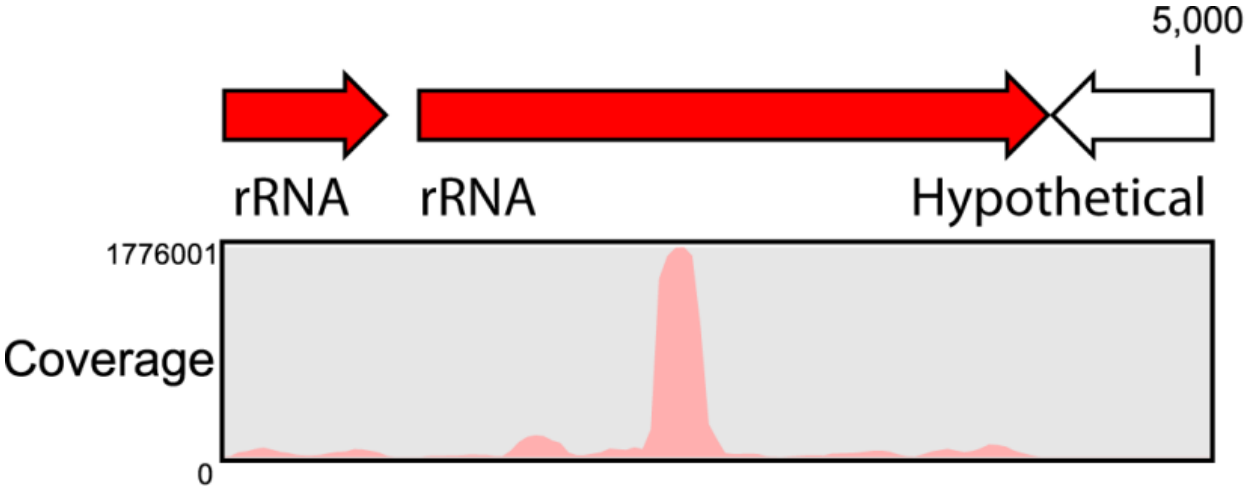

Figure 8. RNA-Seq coverage of the most highly mapped region. A region with the most mapped reads belongs to contig00001 and a representative alignment trace is shown from 829 12H.

Table 1

	Total Reads	Reads mapped	Reads mapped to non-ribosomal genes
828 12H	31,484,606	3,247,784	487
829 24H	31,203,286	3,570,536	350
8156 12H	37,081,503	4,376,634	793
8156 24H	32,744,930	2,316,583	352
8705 12H	32,951,191	2,938,843	277
8705 24H	66,742,126	7,400,058	725
8718 12H	33,124,095	3,314,285	438

Table 1. Mapping analysis of RNA sequencing results.

Table 2

Gene Annotation	8718 12H	8705 12H	829 12H	8156 12H	8156 24H	829 24H	8705 24H
Translation elongation factor Tu	228	72	204	435	149	96	253
Hypothetical (00001)	53	52	15	80	27	36	93
Translation elongation factor G	28	7	35	28	29	20	29
Chaperone protein DnaK	20	19	31	22	16	18	34
Hypothetical (00158_[2])	6	2	36	15	3	27	23
Stage VI sporulation protein D	1	26	3	12	1	16	32
Hypothetical (00204)	4	5	22	11	5	17	21
DNA-directed RNA polymerase β subunit (EC 2.7.7.6)	8	6	6	35	5	8	12
Heat shock protein 60 family chaperone GroEL	8	8	5	29	3	7	5
DNA-directed RNA polymerase β' subunit (EC 2.7.7.6)	1	3	3	13	2	6	12
ATP synthase β chain (EC 3.6.3.14)	3	1	3	5	4	2	6

Table 2. Number of reads for the genes identified in all RNA samples.

Table 3

Gene Annotation	8718 12H	8705 12H	829 12H	8156 12H	8156 24H	829 24H	8705 24H	Total Reads
Translation elongation factor Tu	228	72	204	435	149	96	253	1437
Hypothetical (00001)	53	52	15	80	27	36	93	356
Translation elongation factor G	28	7	35	28	29	20	29	176
Chaperone protein DnaK	20	19	31	22	16	18	34	160
Hypothetical (00158_[2])	6	2	36	15	3	27	23	112
Stage VI sporulation protein D	1	26	3	12	1	16	32	91
Hypothetical (00204)	4	5	22	11	5	17	21	85
DNA-directed RNA polymerase β subunit (EC 2.7.7.6)	8	6	6	35	5	8	12	80
Heat shock protein 60 family chaperone GroEL	8	8	5	29	3	7	5	65
DNA-directed RNA polymerase β' subunit (EC 2.7.7.6)	1	3	3	13	2	6	12	40
Hypothetical (00065_[2])	5	1	7	7	0	9	5	34
DNA-binding protein HBsu	0	2	0	2	11	4	9	28
ATP synthase β chain (EC 3.6.3.14)	3	1	3	5	4	2	6	24
DNA-directed RNA polymerase α subunit (EC 2.7.7.6)	1	1	2	4	0	1	8	17
Small acid-soluble spore protein, γ-type SASP	6	0	4	0	0	0	6	16
NAD-dependent glyceraldehyde-3-phosphate dehydrogenase (EC 1.2.1.12)	5	0	0	10	0	0	0	15
Translation initiation factor 2 (00065)	2	0	2	4	0	4	3	15
Enolase (EC 4.2.1.11)	0	1	1	1	3	3	6	15
Hypothetical (00158_[2])	0	2	4	3	1	0	1	11
ATP-dependent Clp protease, ATP-binding subunit ClpC	0	2	3	2	0	1	1	9
Hypothetical (00120)	0	0	1	2	0	0	6	9
Small, acid-soluble spore protein O	2	0	2	2	1	0	0	7
Multimodular transpeptidase-transglycosylase (PBP1)	0	1	1	1	1	2	1	7
ABC transporter, permease protein	0	1	0	0	1	2	3	7
Serine hydroxymethyltransferase (EC 2.1.2.1)	1	0	0	2	3	0	0	6
Hydrolase (HAD superfamily) (00065)	0	1	2	1	0	1	1	6
Hypothetical (00115_[2])	0	2	0	0	0	0	4	6
Carbamoyl-phosphate synthase large chain (EC 6.3.5.5) (00204)	3	0	0	1	1	0	0	5
RNA polymerase sigma factor	0	0	3	1	0	0	1	5
Fibronectin -binding protein	0	0	2	1	0	1	1	5
Hypothetical (00033)	0	0	1	1	1	1	1	5
ATP-dependent Clp protease ATP-binding subunit ClpX	0	0	1	0	1	0	3	5
Metalloprotease, putative zinc-binding domain	0	2	0	0	0	0	2	4
Cold shock protein CspA	0	0	3	0	1	0	0	4
Exodeoxyribonuclease VII small subunit (EC 3.1.11.6)	0	0	1	1	0	0	2	4
Hypothetical (00115_[2])	0	0	2	0	2	0	0	4
small, acid-soluble spore protein, SspJ family	0	0	0	2	0	2	0	4
YvlB	0	0	1	0	1	1	1	4
Hypothetical (00115_[2])	0	0	1	0	0	3	0	4
Small, acid-soluble spore protein N	0	0	0	4	0	0	0	4
Cell division protein FtsH	2	0	1	0	0	0	0	3
Glutamate transport ATP-binding protein (00115_[2])	2	0	0	1	0	0	0	3
Topoisomerase IV subunit B	2	1	0	0	0	0	0	3
Hypothetical (00204)	1	1	0	1	0	0	0	3
Flagellin protein FlaA (00117)	0	1	1	0	0	0	1	3
Germination (Cortex hydrolysis) and sporulation protein GerM	0	2	0	0	0	1	0	3
Signal recognition particle, subunit Ffh SRP54	0	1	1	0	0	1	0	3
DNA-directed RNA polymerase delta subunit	0	0	1	0	0	0	2	3
Maltose/maltodextrin ABC transporter, substrate binding periplasmic protein MalE	0	1	0	0	0	2	0	3
Pyruvate kinase (EC 2.7.1.40)	0	0	1	0	0	1	1	3
Protein export cytoplasm protein SecA ATPase RNA helicase	0	0	0	1	1	0	1	3
Polyribonucleotide nucleotidyltransferase (EC 2.7.7.8)	0	0	0	1	0	2	0	3
Chromosome partition protein smc	0	0	0	0	0	2	1	3
Carbamoyl-phosphate synthase large chain (EC 6.3.5.5) (00117)	0	2	0	1	0	0	0	3
Delta-1-pyrroline-5-carboxylate dehydrogenase (EC 1.5.1.12)	2	0	0	0	0	0	0	2
Dihydrolipoamide succinyltransferase component (E2) of 2-oxoglutarate dehydrogenase complex	2	0	0	0	0	0	0	2
FIG007042: Hypothetical	2	0	0	0	0	0	0	2
Flagellar hook-associated protein FlgK	2	0	0	0	0	0	0	2
Glutamine synthetase type I (EC 6.3.1.2)	2	0	0	0	0	0	0	2
Hypothetical (00115_[2])	2	0	0	0	0	0	0	2
NADPH dependent preQ0 reductase	2	0	0	0	0	0	0	2

Table 3 (cont.)

anti-sigma factor homolog yrhM	1	0	0	1	0	0	0	2
holin protein	1	0	0	1	0	0	0	2
ABC transporter substrate-binding protein	0	1	0	0	0	0	1	2
Hypothetical (00158_[2])	0	0	1	0	0	0	1	2
GTP-binding protein Era	0	1	0	0	1	0	0	2
ATP-dependent RNA helicase YxiN	0	0	0	1	0	0	1	2
Adenylosuccinate lyase (EC 4.3.2.2)	0	0	1	0	0	1	0	2
Peptidoglycan N-acetylglucosamine deacetylase (EC 3.5.1.-) (00115_[2])	0	0	0	1	1	0	0	2
bacillopeptidase F (00204)	0	0	0	1	0	1	0	2
Serine/threonine protein kinase PrkC, regulator of stationary phase	0	0	0	1	0	1	0	2
3-isopropylmalate dehydrogenase (EC 1.1.1.85)	0	0	0	0	0	2	0	2
5-bromo-4-chloroindolyl phosphate hydrolysis protein	0	0	0	0	0	0	2	2
5'-nucleotidase family protein	0	0	0	0	0	2	0	2
Alanyl-tRNA synthetase (EC 6.1.1.7) (00115_[2])	0	0	0	0	0	1	1	2
Asparagine synthetase [glutamine-hydrolyzing] (EC 6.3.5.4) YisO	0	0	0	0	0	0	2	2
ATP synthase alpha chain (EC 3.6.3.14)	0	0	0	0	1	0	1	2
Chaperone protein DnaJ	0	0	0	0	0	2	0	2
Collagen adhesion protein	0	0	0	0	0	1	1	2
CTP synthase (EC 6.3.4.2)	0	0	0	0	0	0	2	2
Cysteine synthase (EC 2.5.1.47) (00129)	0	0	0	0	1	1	0	2
Dihydrolipoamide acetyltransferase component of pyruvate dehydrogenase complex (EC 2.3.1.12)	0	0	0	0	0	2	0	2
dipeptide ABC transporter (permease) (00068)	0	0	0	0	0	0	2	2
Hypothetical (00021)	0	0	0	0	0	0	2	2
Hypothetical (00067)	0	0	0	0	0	0	2	2
Hypothetical (00117)	0	0	0	0	0	1	1	2
Spore maturation protein (00105)	0	0	0	0	0	0	2	2
Late competence protein ComEC, DNA transport	0	0	0	0	0	0	2	2
Lysine decarboxylase family	0	0	0	0	0	0	2	2
methyl-accepting chemotaxis protein (00158_[2])	0	0	0	0	0	0	2	2
Protein cgeA	0	0	0	0	2	0	0	2
PTS system, mannitol-specific IIB / IIC component (EC 2.7.1.69)	0	0	0	0	0	0	2	2
Purine nucleoside phosphorylase (EC 2.4.2.1) (00012)	0	0	0	0	0	0	2	2
Pyruvate-utilizing enzyme, similar to phosphoenolpyruvate synthase	0	0	0	0	0	0	2	2
RNA polymerase sigma factor SigW	0	0	0	0	2	0	0	2
Small, acid-soluble spore protein P	0	0	0	0	0	0	2	2
Spore coat protein G	0	0	0	0	0	0	2	2
transcriptional regulator of the bltD operon	0	0	0	0	0	0	2	2
Hypothetical (00120)	0	0	0	0	0	0	2	2
ABC superfamily ATP binding cassette transporter, membrane protein	0	2	0	0	0	0	0	2
Acetyl-CoA:acetoacetyl-CoA transferase, beta subunit (EC 2.8.3.8)	0	0	2	0	0	0	0	2
ATP synthase gamma chain (EC 3.6.3.14)	0	0	2	0	0	0	0	2
ATP-dependent Clp protease-like	0	0	1	1	0	0	0	2
Cold shock protein CspD	0	0	2	0	0	0	0	2
Hypothetical (00017)	0	0	1	1	0	0	0	2
DNA gyrase subunit A (EC 5.99.1.3)	0	2	0	0	0	0	0	2
Fe-S oxidoreductase	0	0	2	0	0	0	0	2
Flagellin protein FlaA (00117)	0	0	0	2	0	0	0	2
Gluconate transporter family protein	0	2	0	0	0	0	0	2
GTP-binding protein YqeH, required for biogenesis of 30S ribosome subunit	0	2	0	0	0	0	0	2
Helicase, SNF2/RAD54 family	0	2	0	0	0	0	0	2
Hypothetical (00086)	0	2	0	0	0	0	0	2
Hypothetical (00120)	0	2	0	0	0	0	0	2
Hypothetical (00158)	0	0	0	2	0	0	0	2
Hypothetical (00158_[2])	0	2	0	0	0	0	0	2
Ketol-acid reductoisomerase (EC 1.1.1.86)	0	0	0	2	0	0	0	2
Lipoteichoic acid synthase LtaS Type Ib	0	0	2	0	0	0	0	2
L-lysine aminomutase regulator	0	2	0	0	0	0	0	2
membrane protein, putative (00158_[2])	0	2	0	0	0	0	0	2
Predicted L-lactate dehydrogenase, Fe-S oxidoreductase subunit YkgE	0	2	0	0	0	0	0	2
PTS system, fructose-specific IIA / IIB / IIC (00204)	0	2	0	0	0	0	0	2
Quinolinate phosphoribosyltransferase [decarboxylating] (EC 2.4.2.19)	0	0	0	2	0	0	0	2
Similar to proteins GerPF and GerPA	0	0	0	2	0	0	0	2
Small, acid-soluble spore protein tlp	0	0	2	0	0	0	0	2
Spore coat protein V	0	0	2	0	0	0	0	2
Thiamine-monophosphate kinase (EC 2.7.4.16)	0	0	0	2	0	0	0	2
Transition state regulatory protein AbrB (00129)	0	0	2	0	0	0	0	2
UDP-N-acetylglucosamine 1-carboxyvinyltransferase (EC 2.5.1.7) (00116_[2])	0	0	2	0	0	0	0	2
unknown (00011 11443..12634)	0	0	2	0	0	0	0	2
catalyses ATP-dependent electrogenic Na+ extrusion without mechanistically coupled H+ or K+ uptake (00012)	1	0	0	0	0	0	0	1
Dihydroxy-acid dehydratase (EC 4.2.1.9)	1	0	0	0	0	0	0	1
Phage-like element PBSX protein xkdP	1	0	0	0	0	0	0	1
Transcriptional regulator BkdR of isoleucine and valine catabolism	1	0	0	0	0	0	0	1

Table 3 (cont.)

tRNA-i(6)A37 methylthiotransferase	1	0	0	0	0	0	0	1
2,3-butanediol dehydrogenase, alcohol forming, acetoin-specific	0	0	0	0	0	0	1	1
2,3-dihydroxybenzoate-AMP ligase [bacillibactin] siderophore	0	0	0	0	0	0	1	1
2-amino-3-ketobutyrate coenzyme A ligase (EC 2.3.1.29)	0	0	0	0	0	1	0	1
ABC transporter ATP-binding protein uup	0	0	0	0	0	1	0	1
ABC transporter, ATP-binding protein (00204)	0	0	0	0	0	0	1	1
Acetoin dehydrogenase E1 component alpha-subunit (EC 1.2.4.-) (00041)	0	0	0	0	0	1	0	1
Alanine racemase (EC 5.1.1.1) (00041)	0	0	0	0	1	0	0	1
α-N-arabinofuranosidase 2 (EC 3.2.1.55)	0	0	0	0	0	0	1	1
ATP-dependent RNA helicase	0	0	0	0	0	1	0	1
Cell division protein FtsI [Peptidoglycan synthetase] (EC 2.4.1.129) (00120)	0	0	0	0	0	0	1	1
Cell division protein FtsZ	0	0	0	0	0	1	0	1
Chromosome partitioning protein ParA / Sporulation initiation inhibitor protein Soj	0	0	0	0	0	0	1	1
D-3-phosphoglycerate dehydrogenase (EC 1.1.1.95)	0	0	0	0	0	1	0	1
D-alanyl-D-alanine carboxypeptidase (EC 3.4.16.4) (00105 302765..303966)	0	0	0	0	0	0	1	1
Dehydrosqualene desaturase (EC 1.14.99.-)	0	0	0	0	0	0	1	1
DNA integrity scanning protein disA	0	0	0	0	0	0	1	1
Duplicated ATPase component MtsB of energizing module of methionine-regulated ECF transporter	0	0	0	0	0	0	1	1
Flagellar biosynthesis protein FlhB (00204_[2])	0	0	0	0	0	1	0	1
Glutamate synthase [NADPH] large chain (EC 1.4.1.13)	0	0	0	0	0	0	1	1
Glutamate transport ATP-binding protein (00120 12448..13171)	0	0	0	0	1	0	0	1
Glyceraldehyde-3-phosphate ketol-isomerase (EC 5.3.1.1)	0	0	0	0	0	0	1	1
Hypothetical membrane protein (00067)	0	0	0	0	0	1	0	1
Hypothetical (00012)	0	0	0	0	0	1	0	1
Hypothetical (00012)	0	0	0	0	0	0	1	1
Hypothetical (00026)	0	0	0	0	0	0	1	1
Hypothetical (00026)	0	0	0	0	0	1	0	1
Hypothetical (00033)	0	0	0	0	0	0	1	1
Hypothetical (00068)	0	0	0	0	0	0	1	1
Hypothetical (00105)	0	0	0	0	0	1	0	1
Hypothetical (00115_[2])	0	0	0	0	0	1	0	1
Hypothetical (00134)	0	0	0	0	0	1	0	1
Long-chain-fatty-acid--CoA ligase (EC 6.2.1.3) (00078)	0	0	0	0	0	0	1	1
molybdopterin oxidoreductase	0	0	0	0	0	1	0	1
Nitrite reductase [NAD(P)H] large subunit (EC 1.7.1.4) (00105)	0	0	0	0	0	0	1	1
Nucleoside 5-triphosphatase RdgB (EC 3.6.1.15)	0	0	0	0	0	0	1	1
L-carnitine/choline ABC transporter/permease protein OpuCD	0	0	0	0	0	0	1	1
pectate lyase	0	0	0	0	0	1	0	1
Peptide chain release factor 1	0	0	0	0	0	1	0	1
Phosphate starvation-inducible protein PhoH, predicted ATPase	0	0	0	0	0	1	0	1
Phosphoribosylaminoimidazole-succinocarboxamide synthase (EC 6.3.2.6)	0	0	0	0	0	1	0	1
phytoene dehydrogenase	0	0	0	0	0	1	0	1
Putative deoxyribonuclease YcfH	0	0	0	0	0	0	1	1
Putative toxin component near putative ESAT-related proteins, repetitive (00115_[2])	0	0	0	0	0	1	0	1
RecA protein	0	0	0	0	1	0	0	1
response regulator aspartate phosphatase (00159)	0	0	0	0	1	0	0	1
small, acid-soluble spore protein	0	0	0	0	1	0	0	1
Spore photoproduct lyase	0	0	0	0	1	0	0	1
transcriptional regulator, DeoR family (00155)	0	0	0	0	0	1	0	1
transcriptional regulator, XRE family	0	0	0	0	1	0	0	1
Valyl-tRNA synthetase (EC 6.1.1.9)	0	0	0	0	1	0	0	1
Xylose isomerase (EC 5.3.1.5)	0	0	0	0	0	0	1	1
Zn-finger protein	0	0	0	0	0	0	1	1
2,3-bisphosphoglycerate-independent phosphoglycerate mutase (EC 5.4.2.1)	0	1	0	0	0	0	0	1
Acetyltransferase (EC 2.3.1.-) (00158_[2])	0	1	0	0	0	0	0	1
amino acid ABC transporter ATP-binding protein	0	0	1	0	0	0	0	1
Branched-chain α-keto acid dehydrogenase, E1 component, α subunit (EC 1.2.4.4)	0	1	0	0	0	0	0	1
Cell division protein FtsK (00155)	0	0	1	0	0	0	0	1
conserved Hypothetical (00115_[2])	0	1	0	0	0	0	0	1
DNA gyrase subunit B (EC 5.99.1.3) (00033)	0	0	1	0	0	0	0	1
D-tyrosyl-tRNA(Tyr) deacylase	0	1	0	0	0	0	0	1
Flagellar motor switch protein FliN	0	0	0	1	0	0	0	1
Glutamate N-acetyltransferase / N-acetylglutamate synthase	0	0	1	0	0	0	0	1
Glutamate transport ATP-binding protein (00116_[3])	0	0	0	1	0	0	0	1
Glycine betaine ABC transport system, OpuABC	0	0	0	1	0	0	0	1
glycosyl transferase, group 2 family protein	0	0	1	0	0	0	0	1
Glycyl-tRNA synthetase alpha chain (EC 6.1.1.14)	0	0	0	1	0	0	0	1
GTP pyrophosphokinase (EC 2.7.6.5), (p)ppGpp synthetase I	0	0	0	1	0	0	0	1
Histidine kinase sensor protein	0	0	0	1	0	0	0	1
Hypothetical phagelike protein	0	1	0	0	0	0	0	1
Hypothetical (00012)	0	1	0	0	0	0	0	1

Table 3 (cont.)

Hypothetical (00026)	0	1	0	0	0	0	0	1
Hypothetical (00026)	0	1	0	0	0	0	0	1
Hypothetical (00067)	0	0	0	1	0	0	0	1
Hypothetical (00115_[2])	0	0	0	1	0	0	0	1
Hypothetical (00116_[3])	0	0	0	1	0	0	0	1
Hypothetical (00116_[3])	0	0	1	0	0	0	0	1
Hypothetical (00158_[2])	0	0	1	0	0	0	0	1
Hypothetical (00158_[2])	0	0	1	0	0	0	0	1
Hypothetical (00204)	0	0	0	1	0	0	0	1
Hypothetical (00204)	0	0	1	0	0	0	0	1
Isocitrate dehydrogenase [NADP] (EC 1.1.1.42)	0	0	0	1	0	0	0	1
Isoleucyl-tRNA synthetase (EC 6.1.1.5)	0	0	0	1	0	0	0	1
Long-chain-fatty-acid--CoA ligase (EC 6.2.1.3) (00115_[2])	0	0	1	0	0	0	0	1
Maltose/maltodextrin ABC transporter, permease protein MalF	0	1	0	0	0	0	0	1
Manganese superoxide dismutase (EC 1.15.1.1)	0	0	0	1	0	0	0	1
methyl-accepting chemotaxis protein (00158_[2])	0	0	1	0	0	0	0	1
N-acetylmuramic acid 6-phosphate etherase (EC 4.2.-.-)	0	0	0	1	0	0	0	1
NADPH-dependent glyceraldehyde-3-phosphate dehydrogenase (EC 1.2.1.13)	0	0	1	0	0	0	0	1
NADP-specific glutamate dehydrogenase (EC 1.4.1.4)	0	0	0	1	0	0	0	1
oxidoreductase, short-chain dehydrogenase/reductase family (00105 325783..326560)	0	1	0	0	0	0	0	1
Peptidase T (EC 3.4.11.4)	0	0	0	1	0	0	0	1
Phage-like element PBSX protein xkdK	0	1	0	0	0	0	0	1
Prolyl-tRNA synthetase (EC 6.1.1.15) Bacterial type (00026)	0	1	0	0	0	0	0	1
Protein of unknown function identified by role in sporulation (SpoVG)	0	0	0	1	0	0	0	1
Proton/glutamate symport protein Sodium/glutamate symport protein (00158_[2])	0	0	0	1	0	0	0	1
Putative toxin component near putative ESAT-related proteins	0	0	1	0	0	0	0	1
Replicative DNA helicase (EC 3.6.1.-) (00052)	0	0	1	0	0	0	0	1
Siderophore biosynthesis non-ribosomal peptide synthetase modules /Bacillibactin synthetase component F (EC 2.7.7.-) (00033)	0	0	1	0	0	0	0	1
Spore germination protein GerKA (00116_[2])	0	0	0	1	0	0	0	1
Spore germination protein YpeB	0	1	0	0	0	0	0	1
Transcription antitermination protein NusG	0	0	0	1	0	0	0	1
Transcription-repair coupling factor	0	1	0	0	0	0	0	1
tRNA-specific adenosine-34 deaminase (EC 3.5.4.-)	0	1	0	0	0	0	0	1
Type I restriction-modification system, specificity subunit S (EC 3.1.21.3) (00158_[2])	0	0	1	0	0	0	0	1
Hypothetical (00158_[2])	0	0	1	0	0	0	0	1
YczE	0	0	1	0	0	0	0	1
YdgH	0	0	1	0	0	0	0	1
Zinc ABC transporter, inner membrane permease ZnuB	0	0	1	0	0	0	0	1

Table 3. All genes containing aligned reads

REFERENCES

1. Trompette A., Gollwitzer E.S., Yadava K., Sichelstiel A.K., Sprenger N., Ngom-Bru C., Blanchard C., Junt T., Nicod L.P., Harris N.L., and Marsland B.J. 2014. Gut microbiota metabolism of dietary fiber influences allergic airway disease and hematopoiesis. Nature Med. 20 (2), 159–166.

2. Tam N.K.M., Uyen N.Q., Hong H.A., Duc L.H., Hoa T.T., Serra C.R., Henriques A.O., and Cutting S.M. 2006. The Intestinal Life Cycle of *Bacillus subtilis* and Close Relatives. J. Bact. 188 (7), 2692–2700.

3. Nakano M.M. and Zuber P. 1998. Anaerobic growth of a "strict aerobe" (*Bacillus subtilis*). Ann. Rev. Microbiol. 52, 165 -190.

4. Hoa T.T., Duc L.H., Isticato R., Baccigalupi L., Ricca E., Van P.H., and Cutting S.M. 2001. Fate and Dissemination of *Bacillus subtilis* Spores in a Murine Model. Appl. Environ. Microbiol. 67 (9), 3819–3823.

5. Casula G. and Cutting S.M. 2002. *Bacillus* Probiotics: Spore Germination in the Gastrointestinal Tract. Appl. Environ. Microbiol. 68 (5), 2344–2352.

6. Hong H.A., To E., Fakhry S., Baccigalupi L., Ricca E., and Cutting S.M. 2009. Defining the natural habitat of *Bacillus* spore-formers. Res. Microbiol. 160 (6), 375-379.

7. Sharma R., John S.J., Damgaard M., and McAllister T.A. 2003. Extraction of PCR Quality Plant and Microbial DNA from Total Rumen Contents. BioTechniques 34 (1), 92-97.

8. Laura D. Clements, Uldis N. Streips, and Brian S. Miller. 2002. Differential proteomic analysis of *Bacillus subtilis* nitrate respiration and fermentation in defined medium. PROTEOMICS 12 (2), 1724-1734.

9. Eren A.M., Maignien L., Sul W.J., Murphy L.G., Grim S.L., Morrison H.G., and Sogin M.L. 2013. Oligotyping: differentiating between closely related microbial taxa using 16S rRNA gene data. Methods Ecol. Evol. 4 (12), 1111-1119.

10. Caporaso J.G., Kuczynski J., Stombaugh J., Bittinger K., Bushman F.D., Costello E.K., Fierer N., Gonzalez Pena A., Goodrich J.K., Gordon J.I., Huttley G.A., Kelley S.T., Knights D., Koenig J.E., Ley R.E., Lozupone C.A., McDonald D., Muegge B.D., Pirrung M., Reeder J., Sevinsky J.R., Turnbaugh P.J., Walters W.A., Widmann J., Yatsunenko T., Zaneveld J., and Knight R. 2010. QIIME allows analysis of high-throughput community sequencing data. Nature Methods 7 (5), 335-336.

11. Edgar R.C. 2010. Search and clustering orders of magnitude faster than BLAST. Bioinformatics. 26(19), 2460-2461.

12. Altschul S.F., Gish W., Miller W., Myers E.W., and Lipman D.J. 1990. Basic local alignment search tool. J. Mol. Biol. 215 (3), 403-410.

13. Caporaso J.G., Bittinger K., Bushman F.D., DeSantis T.Z., Andersen G.L., and Knight R. 2010. PyNAST: a flexible tool for aligning sequences to a template alignment. Bioinformatics. (26), 266-267.

14. DeSantis T.Z., Hugenholtz P., Larsen N., Rojas M., Brodie E.L., Keller K., Huber T., Dalevi D., Hu P., and Andersen G.L. 2006. Greengenes, a chimera-checked 16S rRNA gene database and workbench compatible with ARB. Appl. Environ. Microbiol. 72 (7), 5069-5072.

15. McDonald D., Price M.N., Goodrich J., Nawrocki E.P., DeSantis T.Z., Probst A., Andersen G.L., Knight R. and Hugenholtz P. 2012. An improved Greengenes taxonomy with explicit ranks for ecological and evolutionary analyses of bacteria and archaea. ISME J. 6 (3), 610–618.

16. Werner J.J., Koren O., Hugenholtz P., DeSantis T.Z., Walters W.A., Caporaso J.G., Angenent L.T., Knight R., and Ley R.E. 2012. Impact of training sets on classification of high-throughput bacterial 16S rRNA gene surveys. ISME J. (6), 94-103.

17. Wang Q., Garrity G.M., Tiedje J.M., and Cole J.R. 2007. Naive Bayesian classifier for rapid assignment of rRNA sequences into the new bacterial taxonomy. Appl. Environ. Microbiol. 73 (16), 5261-5267.

18. Stamatakis A. 2006. RAxML-VI-HPC: Maximum Likelihood-based Phylogenetic Analyses with Thousands of Taxa and Mixed Models. Bioinformatics. 22 (21), 2688-2690.

19. Lozupone C. and Knight R. 2005. UniFrac: a new phylogenetic method for comparing microbial communities. Appl. Environ. Microbiol. 71 (12), 8228-8235.

20. Vazquez-Baeza Y., Pirrung M., Gonzalez A., and Knight R. 2013. Emperor: A tool for visualizing high-throughput microbial community data. Gigascience. 2 (1), 16.

21. Turnbaugh P.J., Ley R.E., Mahowald M.A., Magrini V., Mardis E.R., and Gordon J.I. 2006. An obesity-associated gut microbiome with increased capacity for energy harvest. Nature. 444 (7122), 1027-31.

22. Atrih, A., Zollner P., Allmaier J., and Foster S.J. 1996. Structural analysis of Bacillus subtilis 168 endospore peptidoglycan and its role during differentiation. J Bacteriol. 178 (21), 6173-6183.

23. Popham D. L., Helin J., Costello C.E., and Setlow P. 1996. Analysis of the peptidoglycan structure of Bacillus subtilis endospores. J. Bacteriol. 178(22), 6451-6458.

24. Warth, A. D. and J. L. Strominger. 1972. Structure of the peptidoglycan from spores of Bacillus subtilis. Biochemistry. 11, 1389-1396.

25. Warth A. D. and Strominger J.L. 1971. Structure of the peptidoglycan from vegetative cell walls of Bacillus subtilis. Biochemistry. 10 (22), 4349-4358.

26. Warth, A. D. and J. L. Strominger. 1969. Structure of the peptidoglycan of bacterial spores: occurrence of the lactam of muramic acid. Proc. Natl. Acad. Sci. USA. 64 (2), 528-535.

27. Gerhardt P, Marquis R.E. 1989. Spore thermoresistance mechanisms. In: Smith I., Slepecky R.A. and Setlow P., eds. *Regulation of procaryotic development: structural and functional analysis of bacterial sporulation and germination.* Washington, DC: American Society for Microbiology; 43-63.

28. Reineke K., Mathys A., Heinz V., and Knorr D. 2013. Mechanisms of endospore inactivation under high pressure. Trends Microbiol. 21 (6), 296–304.

29. Fuller, R. 1989. A review: Probiotics in man and animals. J Appl. Bacteriol. 66 (5), 365-378.

30. Metchnikoff. (1910). *The Prolongation of Life. Optimistic Studies.* New York: G P Putnam's Sons. 96.

31. Nurmi E, Rantala M.1973. New aspects of Salmonella infection in broiler production. Nature. 241 (5386), 210-211.

32. Seo J.K., Kim S.W., Kim M.H., Upadhaya S.D., Kam D.K., Jong K.H. 2010. Direct-fed Microbials for Ruminant Animals. Asian Australas. J. Anim. Sci. 23 (12), 1657-1667.

33. Jung C., Hugot J.P., and Barreau F. 2010. Peyer's Patches: The Immune Sensors of the Intestine. International Journal of Inflammation2010 (2010): 823710. *PMC*. Web. 27 Apr. 2015.

Oorrrrrr Jung C, Hugot J-P, Barreau F. Peyer's Patches: The Immune Sensors of the Intestine. *International Journal of Inflammation*. 2010 (2010), 823710.

34. Ghorbani G.R., Morgavi D.P., Beauchemin K.A. and Leedle J.A. 2002. Effects of bacterial direct-fed microbials on ruminal fermentation, blood variables, and the microbial populations of feedlot cattle. J. Anim. Sci. 80 (7), 1977-1985.

35. Krehbiel C. R., Rust S.R., Zhang G., and Gilliland S.E. 2003. Bacterial direct-fed microbials in ruminant diets: Performance response and mode of action. J. Anim. Sci. 80 (1), 120-132.